

Pore-Scale Flow Characterization of Polymer Solutions in Microfluidic Porous Media

Christopher A. Browne¹, Audrey Shih¹, and Sujit S. Datta^{1,*}

¹Chemical and Biological Engineering, Princeton University, Princeton, NJ

*Email: ssdatta@princeton.edu

9 September 2019

Abstract

Polymer solutions are frequently used in enhanced oil recovery and groundwater remediation to improve the recovery of trapped non-aqueous fluids. However, applications are limited by an incomplete understanding of the flow in porous media. The tortuous pore structure imposes both shear and extension, which elongates polymers; moreover, the flow is often at large Weissenberg numbers Wi at which polymer elasticity in turn strongly alters the flow. This dynamic elongation can even produce flow instabilities with strong spatial and temporal fluctuations despite the low Reynolds number Re . Unfortunately, macroscopic approaches are limited in their ability to characterize the pore-scale flow. Thus, understanding how polymer conformations, flow dynamics, and pore geometry together determine these non-trivial flow patterns and impact macroscopic transport remains an outstanding challenge. Here, we describe how microfluidic tools can shed light on the physics underlying the flow of polymer solutions in porous media at high Wi and low Re . Specifically, microfluidic studies elucidate how steady and unsteady flow behavior depends on pore geometry and solution properties, and how polymer-induced effects impact non-aqueous fluid recovery. This work provides new insights for polymer dynamics, non-Newtonian fluid mechanics, and applications such as enhanced oil recovery and groundwater remediation.

1 Motivation

Dissolving high molecular weight polymers in water increases the fluid viscosity and, for sufficiently concentrated solutions, imparts new elastic properties. These effects can dramatically alter flow behavior, with important consequences in biological systems (e.g. pathogen clearance by mucus in the lungs), industrial applications (e.g. spinning and casting materials), and microfluidic devices (e.g. mixing for lab-on-a-chip applications). They are also frequently harnessed to improve enhanced oil recovery (EOR)¹ and groundwater remediation.² In these cases, an injected polymer solution must navigate a disordered porous medium, such as a reservoir rock or a subsurface aquifer, and displace trapped non-aqueous fluids such as oil or contaminants from the pore space, enabling them to be recovered downstream. In addition to approaches such as particle, surfactant, and foam injection,^{3–7} polymer injection is emerging as an attractive approach to EOR and groundwater remediation for three key reasons: (i) Polymers can yield increased fluid recovery compared to water, (ii) Polymers are often more affordable than other additives such as polymer nanoparticles and specialized surfactants, and (iii) Because polymers impart new rheological properties to the fluid, they can give rise to new flow behaviors that can be combined with other techniques such as particle or surfactant injection. Being able to predict and control how macroscopic process variables like fluid pressure and total recovery depend on polymer solution properties and injection conditions is therefore of key practical and economic importance.

These variables are typically characterized at the macroscopic scale through measurements of pressure drop and fluid flow rate in sand packs, core samples, or entire formations. These measurements are then interpreted via Darcy’s law: $|\Delta P| = \eta_{\text{app}}(Q/A)L/k$, where ΔP is the pressure drop across a length L of the porous medium, Q is the volumetric flow rate through a cross-sectional area A , k is the medium permeability, which depends on the pore space geometry and amount of fluid trapping, and η_{app} is the ‘apparent viscosity’ of the polymer solution. Such studies provide important empirical measurements of η_{app} , which reflects the combined influence of different pore-scale flow behaviors. Intriguingly, η_{app} is often found to increase abruptly above a threshold flow rate.⁸ This increase in flow resistance has in turn been linked to increased recovery of trapped non-aqueous fluid,^{9–14} challenging conventional belief that polymers cannot appreciably improve recovery.^{1,15} However, despite its strong impact on EOR and groundwater remediation processes, the reason for this increased flow resistance and the concomitant increase in fluid recovery is still a puzzle. Many mechanisms have been proposed: resistance to polymer elongation,^{16,17} permeability reduction via polymer adsorption,^{18,19} suppressed breakup of the trapped fluid,²⁰ and the onset of unsteady flow fluctuations.^{14,21–24} In practice, multiple such mechanisms may be simultaneously at play.

Unfortunately, macroscopic transport measurements do not provide access to the underlying flow behavior due to the opacity of typical 3D media. As a result, the conditions under which these mechanisms may arise are unknown. X-ray scanning and nuclear magnetic resonance measurements can provide valuable information of 3D structure and macroscopic flow, but cannot resolve pore-scale flow details with sufficient spatial or temporal resolution.^{25–35} Flow imaging in mesoscale model systems provides some key insights into the flow structure,^{36–39} but such devices cannot recapitulate the small length scales that characterize real-world porous media (Table 1). As a result, these approaches are often subject to inertial

effects, which typically do not arise during EOR and groundwater remediation and instead complicate the interpretation of laboratory measurements. As a result, the mechanisms by which polymer solutions potentially increase flow resistance and enhance fluid recovery remain poorly understood and hotly debated.^{40–42}

In this Review, we describe how microfluidic tools can shed light on this puzzle. First, we summarize how microfluidics provides a straightforward means to directly visualize flow behavior in model porous media (§2). Next, we summarize the essential flow properties of bulk polymer solutions (§3). We then review the body of work using microfluidics to study how polymer dynamics and porous medium geometry together determine steady (§4.1) and unsteady (§4.2–5) flow behavior. We then describe recent efforts applying these insights to understand the mechanisms underlying enhanced fluid recovery due to polymer solutions (§6). Finally, we highlight new opportunities for microfluidics in elucidating polymer solution flow in porous media, with consequences for EOR, groundwater remediation, and other emerging applications (§7).

2 Microfluidic models of porous media

The porous media relevant to EOR and groundwater remediation are typically dense packings of water-wet soil, rock, and mineral grains. The resulting pore spaces are highly heterogeneous and tortuous, with successive contractions and expansions known as pore throats and pore bodies, respectively; the pore throat diameters L_t typically range from ~ 100 nm to $10\text{ }\mu\text{m}$ (Figure 1a) while the pore body diameters L_b are typically ≈ 2 to 5 times larger. During injection, a polymer solution is forced to flow through this pore space. The interstitial injection speed $U \equiv Q/\phi A$, where $\phi \approx 0.1$ to 0.4 is the medium porosity, is limited by the ability to apply a sufficiently large fluid pressure drop; thus, interstitial flow speeds typically range between ~ 0.01 and $100\text{ }\mu\text{m/s}$.^{14,43} We summarize these pore-scale parameters in Table 1. Under these conditions, inertia is always absent: the fluid *Reynolds number* $\text{Re} \equiv \rho U L_t / \eta$, which describes the relative importance of inertial to viscous stress for a fluid with density ρ and shear viscosity η , ranges from $\sim 10^{-11}$ to $10^{-3} \ll 1$ (Table 2). Thus, Newtonian fluids exhibit laminar, steady-state flow. By contrast, polymer solutions can exhibit dramatic flow instabilities in this range of Re due to the influence of the fluid elasticity, as we describe further in §5.

Microfluidics provides the ability to design pore space geometries at length scales relevant to real-world porous media, with spatial resolutions as small as ~ 50 nm. Furthermore, photolithography allows for fabrication of a wide range of complex microfluidic designs that can recapitulate pore space geometries, and can be used to systematically test the influence of different geometric parameters on flow behavior.⁴⁴ Finally, microfluidic devices can be designed to be optically transparent, enabling pore-scale flow visualization using optical imaging. Such platforms thus enable systematic characterization of the flow patterns, polymer elongation dynamics, and flow fluctuations during polymer solution flow through model porous media. 2D microfluidic channels are typically fabricated in PDMS (polydimethylsiloxane) using soft photolithography, or in hard polymeric resins using 3D-printing.⁴⁵ These channels are then sealed against a glass slide to allow imaging of the flow using tracers via optical microscopy.⁴⁶ Designs of varying complexity can then be used to either simplify or

closely mimic the complex geometry of real-world porous media (Figure 1).

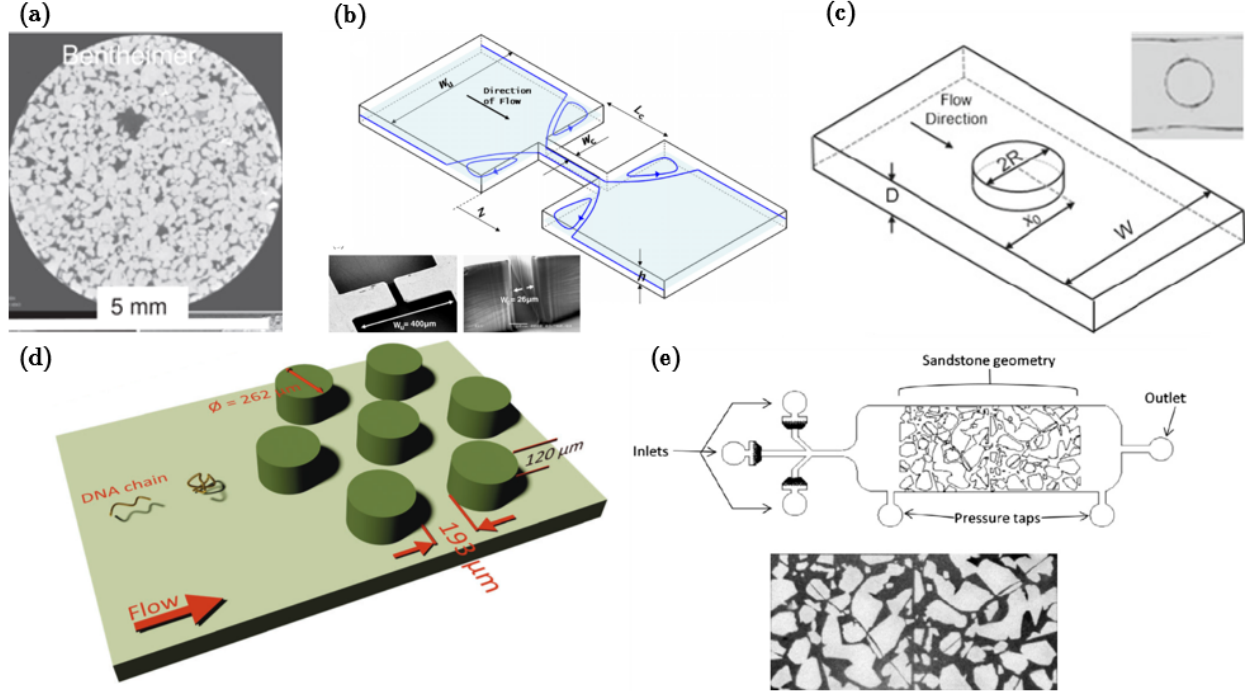


Figure 1: (a) X-ray CT scan of Bentheimer sandstone, a typical rock encountered in EOR,⁴⁷ for comparison to several PDMS microfluidic model porous media. Copyright 2013, Elsevier; reprinted with permission. (b) Sudden flow constriction models the expansion-contracting geometry of the pore space.⁴⁸ Copyright 2007, Elsevier; reprinted with permission. (c) A channel-centered cylinder models the impinging flow on a curved grain; W is the channel width, R is the cylinder radius, x_0 is the cylinder position, and D is the channel height. Inset shows an photograph of a channel molded from a photolithographic cast.⁴⁹ Copyright 2013, Springer; reprinted with permission. (d) A 2D array of cylindrical pillars to model a porous medium.⁵⁰ Copyright 2017, Royal Society of Chemistry; reprinted with permission. (e) A microfluidic device with a disordered 2D pore space, for more realistic modeling of a sandstone network.⁵¹ Copyright 2013, Elsevier; reprinted with permission.

Table 1: Table of key descriptors of polymer solution flow in real-world porous media.

Parameter	Order-of-magnitude range
Pore throat diameter L_t	0.1 to 10 μm
Pore body diameter L_b	0.2 to 50 μm
Fluid viscosity η	1 to 100 cP
Interstitial flow speed U	10^{-2} to 10^2 $\mu m/s$
Shear rate $\dot{\gamma} \sim U/L_t$	10^{-3} to 10^3 s^{-1}
Pore residence time $\tau_{res} \sim L_b/U$	2×10^{-3} to 5×10^3 s
Polymer relaxation time λ	10^{-2} to 10^2 s

The simplest representation of a pore is a sudden rectangular constriction, which captures the expansion and contraction of the tortuous pore space (Figure 1b). Alternatively, the flow can be treated as impinging directly onto a curved grain, which can be represented as a channel-centered cylinder (Figure 1c). Both the rectangular constriction and channel-

Table 2: Table of key dimensionless parameters characterizing polymer solution flow in porous media. ρ is the fluid density, U is the interstitial flow speed, L_t is the pore throat diameter, η is the fluid shear viscosity, N_1 is the first normal stress difference, σ is the shear stress, λ is the polymer relaxation time, $\dot{\gamma}$ is the shear rate, τ_{res} is the polymer residence time in a pore, ϕ is the medium porosity, and γ is the aqueous-nonaqueous fluid interfacial tension.

Parameter	Definition	Interpretation	Range
Reynolds	$\text{Re} \equiv \rho U L_t / \eta$	inertial stress / viscous stress	10^{-11} to 10^{-3}
Weissenberg	$\text{Wi} \equiv N_1 / 2\sigma \approx \lambda \dot{\gamma}$	elastic stress / viscous stress	10^{-5} to 10^5
Deborah	$\text{De} \equiv \lambda / \tau_{\text{res}}$	polymer relaxation time / residence time	2×10^{-6} to 5×10^4
Capillary	$\text{Ca} \equiv \eta U \phi / \gamma$	pore-scale viscous stress / capillary pressure	10^{-10} to 10^{-3}

centered cylinder can be repeated in a linear series to model flow through multiple successive pores. More complex designs probe the spatial effects in a porous network by placing obstacles (square, circular, or triangular) on a 2D lattice (Figure 1d). At an even higher level of complexity, 2D sections of real porous media can be used to fabricate disordered porous networks (Figure 1e). While all of these designs are two-dimensional, and hence underrepresent the connectivity and complexity of the full three-dimensional pore space of real-world media, they provide valuable insights into polymer solution flow—specifically, how it is influenced by flow conditions and the geometry of the pore space.

3 Steady Flow Properties of Bulk Polymer Solutions

3.1 Shear and Extensional Viscosity

EOR and groundwater remediation efforts increasingly utilize high molecular weight (typically \sim MDa) water-soluble polymers, such as xanthan gum and polyacrylamide derivatives. In practice, these polymers are typically added to water at concentrations $C \sim 10$ to 1000 ppm. These concentrations range from the dilute regime—in which the different polymer chains are well-separated and do not overlap—to the semi-dilute regime in which neighboring chains begin to interact; the transition between these two regimes is given by the “overlap concentration” C^* .

One standard method of characterizing the solution flow behavior is using a shear rheometer, which quantifies the dependence between the shear stress σ and the shear rate $\dot{\gamma}$: $\sigma = \eta_s(\dot{\gamma})\dot{\gamma}$, where the non-Newtonian shear viscosity η_s is shear rate-dependent. In particular, these solutions are typically shear thinning. The addition of polymers monotonically increases the zero-shear viscosity of the solution; as shear rate increases, the viscosity decreases, ultimately approaching the background solvent viscosity. This shear rate-dependence is often modeled as a power law for ease, or with the Carreau-Yasuda model, which provides an analytical fit that is often used in numerics and simulations.^{53,54} However, when the polymer solution is highly dilute, or the background solvent is highly viscous, shear-thinning is typically ignored. The solution—termed a Boger fluid—then has a nearly constant shear viscosity over a broad range of shear rates. Interestingly, some simulations suggest that shear-

thinning effects are often unimportant in polymer solution flow through a porous medium, and flow behaviors are primarily determined by the coupling between pore space geometry and the elastic properties of the fluid.⁵⁵ Others, however, contend that shear-thinning effects dominate the flow behavior.⁵⁶

Extensional flows also arise as the fluid traverses successive expansions and contractions in the pore space. This form of flow produces an additional deviation from the Newtonian viscosity in the form of an extensional viscosity, which is absent in Newtonian fluids under typical conditions: $\eta_e = \sigma_e / \dot{\epsilon}$, where σ_e is the extensional stress and $\dot{\epsilon}$ is the extension rate. For rigid polymers, this extensional viscosity depends on concentration and polymer aspect ratio, the longest dimension of the rod-shaped polymer divided by its dimension across.⁵⁷ For polyelectrolytes, the extensional viscosity can also depend sensitively on salt concentration, the valency of the salt ions, and the particular cations and anions that associate with the chain.^{58–60} Measuring these effects can be challenging, however: most rheometers inherently have shear, making it difficult to differentiate the role of non-Newtonian shear and extensional viscosity. Extensional viscosity can be estimated using opposing jet flow, but it is again difficult to remove the effects of shear. Furthermore, these experiments inherently suffer from inertial effects due to their macroscopic scale.^{61,62} In some cases, the extensional viscosity can be estimated by tracking the pinch-off dynamics of thin fluid filaments, using a model that describes the balance between capillary and viscous effects.^{63,64}

By enabling the design of channels that generate flows with pure extension, microfluidics provides a valuable platform for accurate measurements of extensional viscosity.⁶⁵ For example, stagnation point flows can provide pure planar extension with no shear or inertial effects, allowing direct measurement of the extensional viscosity.⁶⁶ Channels with hyperbolic constrictions can also be designed to minimize shear effects;⁵² pressure drop measurements across the constriction, corrected for shear contributions, then provide a direct mea-

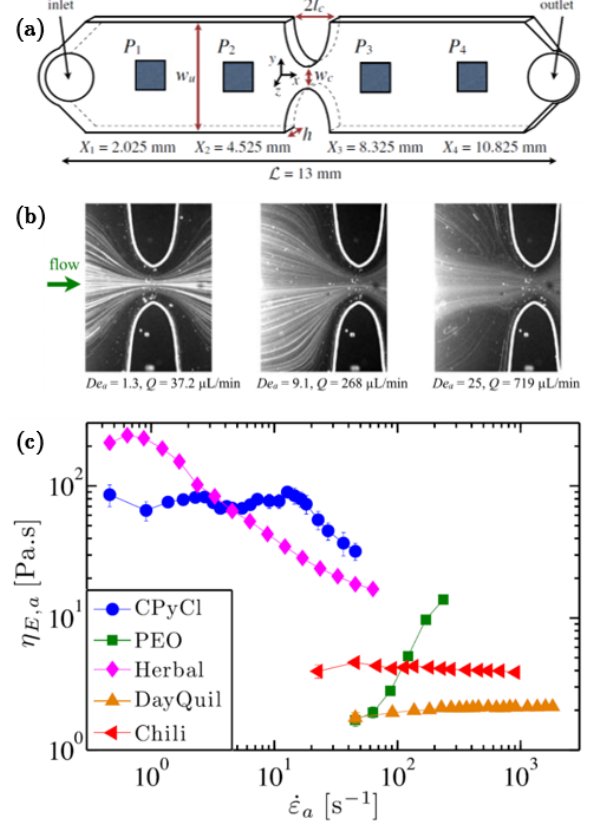


Figure 2: (a) Microfluidic channel with hyperbolic constriction for extensional rheometry. The expansion and contraction widths are $w_u = 2920 \mu\text{m}$ and $w_c = 400 \mu\text{m}$. (b) Streakline images of flow for 3000 ppm of 2 MDa PEO (a flexible polymer) using seed tracer particles; at the highest flow rate large eddies form in the corners leading into the constriction. (c) Extensional rheology for several different solutions measured with hyperbolic microchannel. CPyCl is a worm-like micelle solution composed of 100 mM cetylpyridinium chloride and 60 mM sodium salicylate; PEO is a flexible polymer; Herbal is a commercially available surfactant solution of SDS-SLES; DayQuil is a commercially available solution of CMC, a rigid polymer; Chili is a commercially available solution of xanthan, a semi-rigid polymer.⁵² Copyright 2013, Springer; reprinted with permission.

sure of the extensional viscosity (Figure 2). Other microfluidic designs use the breakup of aqueous droplets in an oil sheath fluid; the extensional viscosity of the polymer solution can then be obtained from the filament thinning dynamics.^{67–69} Intriguingly, such microfluidic experiments have revealed that for sufficient extension rates, the extensional viscosity can abruptly increase—similar to transport measurements on bulk porous media⁷⁰—suggesting a potential contribution to the increased macroscopic flow resistance.

3.2 Quantifying flow-induced deformations

For both shear-thinning and Boger polymer solutions, elastic effects arise from the deformations of the individual polymer chains. For example, shear and extensional flows can force the chains to elongate; this elongation then relaxes over a time scale λ . In certain cases this relaxation can be slow, leading to “memory” of past deformation in the form of retained strain. These fluids are therefore viscoelastic, and exhibit many unusual phenomena that have been studied extensively: rod climbing, die swell, elastic recoil, tubeless siphoning, pressure hole errors, enhanced vortices at contractions, negative wakes, reduction of turbulent drag, and modified jet breakup.⁷¹

This strain retention can be described using constitutive laws that track the accumulation, dissipation, and advection of polymer strain under flow; prominent examples include the Upper Convected Maxwell, Oldroyd-B, and FENE-P models.⁷¹ The Upper Convected Maxwell model gives the fluid stress as a linear combination of a Hookean elastic solid and a Newtonian viscous fluid, with the added consideration that polymer strain is advected by the fluid flow. The Oldroyd-B model gives a more sophisticated treatment of polymers as infinitely extensible linear springs, which couple to the bulk fluid through a relaxation time and a retardation time. The FENE-P model (Finite-Extensibility non-linear Elastic model developed by Peterlin) resolves the non-physical feature of infinite chain extensibility by incorporating a non-linear diverging force needed to extend a polymer to its full contour length.⁷²

Though tracking polymer strain can be computationally challenging, these physical effects can also be captured by two dimensionless parameters that quantify the characteristic amount of chain stretching in a given flow. The *Weissenberg number* indicates the relative magnitude of elastic stresses, quantified by the first normal stress difference N_1 , to viscous stresses, quantified by the shear stress σ :

$$\text{Wi} \equiv \frac{N_1(\dot{\gamma})}{2\sigma(\dot{\gamma})} \approx \lambda\dot{\gamma}.$$

The factor of 1/2 arises from the Oldroyd-B constitutive model; some researchers omit this factor for simplicity, to obtain an order-of-magnitude estimate. The normal stress difference N_1 arises from the stretching of polymer molecules under curved streamlines, which generates a radially inward tension; both N_1 and σ thus depend on the shear rate $\dot{\gamma}$ and can be measured using bulk rheology. A large value of Wi indicates that elastic effects are important, and is generally associated with large amounts of chain extension.

The approximate form on the right hand side of the above equation is Weissenberg’s initially proposed definition,⁷³ but is only used when the fluid rheology is unknown. In this

case, λ is an appropriately chosen relaxation time of the polymer, commonly chosen to be the longest Rouse time, which describes the diffusion of the individual polymer segments but neglects hydrodynamic interactions between them.⁷⁴ However, other experimental measures can be used as well, such as the Zimm relaxation time that also incorporates hydrodynamic interactions between segments.⁷⁵ This timescale is compared with the shear deformation time scale $\dot{\gamma}^{-1}$; however, this value can be replaced by the extensional time scale $\dot{\epsilon}^{-1}$ in the case of extensional flow, giving the extensional $Wi_e \equiv \lambda \dot{\epsilon}$.

Polymers used in EOR and groundwater remediation have λ ranging from $\sim 10^{-2}$ to 10^2 s;¹⁴ moreover, estimating the characteristic deformation rate as the pore flow speed divided by the pore dimension yields a shear rate ranging from $\sim 10^{-3}$ to 10^3 s⁻¹. Thus, flow in a porous medium can be characterized by a broad range of Wi between $\sim 10^{-5}$ and 10^5 (Table 2), indicating that in many cases shear and extensional forces due to flow through the tortuous pore space can extend polymer chains. Elastic effects can therefore play a considerable role.

Another common dimensionless parameter is the *Deborah number*. Though often used interchangeably with Wi , De compares the polymer relaxation time to a flow residence time scale τ_{res} , and not the deformation time scale:^{76,77}

$$De \equiv \frac{\lambda}{\tau_{\text{res}}}.$$

Thus, a large value of De indicates that the polymer chains are being strained over timescales much shorter than their relaxation time—hence, the flow drives them away from their equilibrium state. Indeed, exploring the rheology of polymer solutions in the regime of intermediate and large Deborah numbers is an active area of research.^{78,79} In laboratory extension experiments (§4.2) this flow residence time represents the duration over which a stress is applied. In a tortuous pore space, this residence time is given by the transit time between successive pore throat constrictions $\tau_{\text{res}} \sim L_b/U$; as a result, De can range between $\sim 10^{-6}$ and 10^5 (Table 2).

4 Steady Flow of Polymer Solutions in Porous Media

4.1 Extensional Effects in Bulk Porous Media

Most polymer solutions applied in EOR and groundwater remediation are shear-thinning or Boger fluids; thus, extensional effects resulting from flow through the expanding and contracting pore space are thought to be the primary cause of the increased macroscopic flow resistance observed in bulk porous media.⁸⁰ This increased macroscopic flow resistance can arise from extensional flow in several different ways.

First, for the case of semi-rigid and rigid polymers—such as xanthan, carboxymethylcellulose (CMC), and polyimide—flow imaging in mesoscale setups has revealed the the generation of large corner eddies upstream and downstream of sudden constrictions.^{36,37} Eddies are caused by the preferential alignment of polymers entering the constriction to minimize the extensional stress associated with chain misalignment.^{38,39,57} Given these results, the formation of eddies—which pose an additional source of dissipation and thus contribute to

the macroscopic pressure drop³⁹—may be expected in the many expansions and contractions of a real 3D porous medium. However, this hypothesis remains to be explored.

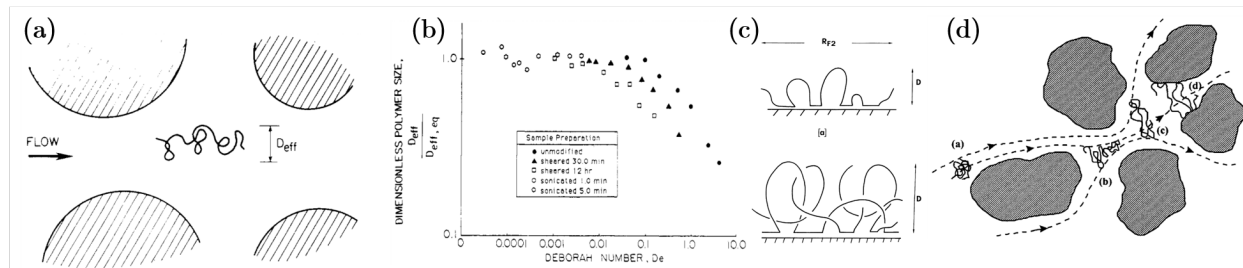


Figure 3: (a) The extensional flow in porous media elongates flexible polymers.⁸¹ Copyright 1989, American Chemical Society; reprinted with permission. (b) This effect can be measured in chromatographic columns because of the reduced effective size D_{eff} which reduces the column transit time; higher Wi_e (termed De here) elongate polymers more, decreasing the effective size.⁸¹ Copyright 1989, American Chemical Society; reprinted with permission. (c) Elongated chains can adsorb onto pore walls because of the increased number of contact points; hanging tails and loops can further entangle polymers at the wall.⁸² Copyright 1976, EDP Sciences; reprinted with permission. (d) In low-permeability pores, extended polymers can bridge pore throats during adsorption, leading to clogging and flow redirection.⁸³ Copyright 2001, Elsevier; reprinted with permission.

Second, for the case of flexible polymers—such as polyacrylamide derivatives, poly(ethylene oxide), and DNA—extensional flows can stretch the individual chains in addition to orienting them (Figure 3a).^{81,84} This change in polymer conformation can be indirectly deduced for flow through a porous medium using transit time measurements: the transit time of a polymer decreases as it elongates. Thus, measurements of polymer transit time for different imposed flow rates, corresponding to different characteristic extensional rates $\dot{\epsilon}$, provide a measure of polymer elongation.⁸¹ These measurements elegantly reveal that flexible polymers experience a coil-stretch transition, abruptly elongating above a threshold $Wi_e \sim 0.5$ (Figure 3b), in agreement with kinetic dumbbell extension theory and microfluidic studies of the coil-stretch transition⁸⁵ as detailed further in §4.2. Polymers take a finite time to reach these equilibrium extensions, which can lead to transient effects as discussed further in §5 for fast flows of high-molecular weight polymers in tortuous porous media.

This flow-induced elongation can have important consequences for pore-scale and macroscopic transport. For example, as chains elongate, they can adsorb irreversibly onto pore walls, which in some cases leads to transient flow redirection or clogging. Coiled polymers typically have small binding energies, but the higher contact area of an elongated polymer produces strong, irreversible binding (Figure 3c).^{82,86,87} Adsorbed polymer layers can constrict pores and generate additional flow resistance (Figure 3d), potentially generating higher viscous pressure drops or redirecting the flow to bypassed regions, thereby promoting displacement and recovery of a trapped non-aqueous fluid.^{18,19,83,88,89} However, in high permeability reservoirs—where polymers have been successfully implemented—the typical thickness of adsorbed layers measured in experiments is too thin to dramatically alter flow resistance and fluid recovery.⁹⁰ This observation suggests that adsorption may play a key role, but cannot fully explain increased flow resistance or enhanced fluid recovery observed in bulk porous media.

Another consequence of flow-induced elongation is an increase in the extensional viscosity, and hence flow resistance, due to the polymer chains resisting elongation.^{16,17} The onset of

elongation in packed columns⁸¹ coincides roughly with the critical shear rate for the excess resistance observed in model porous constrictions.^{91,92} Theoretical work⁹³ was able to match this abrupt increase in extensional viscosity⁹⁴ to the rapid coil-stretch transition,⁹⁵ indicating that polymer elongation is directly responsible for this increased resistance. Fully capturing the physics of this process requires an understanding of the molecular details of polymer elongation; thus, microfluidic tools have been used to investigate the elongation dynamics of single chains. Indeed, simulations in porous media geometries exhibit similar increases in flow resistance, but only when using a polymer constitutive law that explicitly tracks extensional strain such as Oldroyd-B or FENE-P, highlighting the importance of polymer elongation.^{96,97} However, simulations applying these constitutive laws to complex porous geometries cannot fully reproduce the experimentally observed increase in flow resistance,⁹⁸ suggesting that other dissipative processes arise in these flows, as we describe further in §5.

4.2 Elongation Dynamics in Microfluidic Devices

Microfluidic experiments provide a straightforward way to probe the elongation dynamics of polymers in extensional flows. These studies typically employ fluorescently-labeled DNA whose molecular weight can be tuned by harvesting it from different bacteriophage sources or by using restriction endonucleases. This capability allows for direct visualization of single polymer conformations.^{95,99–102} For example, single molecules of DNA can be trapped at the stagnation point in a microfluidic cross-slot channel, enabling the dynamics of elongation to be monitored as the extensional flow is varied.^{103,104} Additionally, the DNA can be embedded within a background polymer solution, acting as a probe of the polymer conformations in the more concentrated solution.^{105,106}

In general, a polymer chain’s equilibrium elongation increases monotonically with Wi_e , transitioning gradually from a more coiled state at $Wi_e = 0$ to a more stretched state at higher $Wi_e \gtrsim 0.5$. The chain length eventually plateaus as it approaches the contour length, which is the maximum elongation possible.⁷¹ For longer chains, however, the transition from a coiled to a stretched state is sharp, yielding a nearly-discontinuous first-order transition.^{107–111} In this case, the chain remains nearly coiled at low Wi_e , showing only a slight increase in its equilibrium elongation as Wi_e is increased. Above a threshold $Wi_e \sim 0.5$, however, the equilibrium elongation increases sharply with Wi_e . Further increases in Wi_e generate only a gradual increase in elongation as the chain approaches its contour length. This behavior allows a simple approximation of the conformation of large polymers: below $Wi_e < 0.5$ chains are fully coiled, and above $Wi_e > 0.5$ chains are fully stretched, known as the coil-stretch transition.

However, for large polymers in highly viscous solvents, the equilibrium length is not uniquely determined by Wi_e —it also depends on the initial chain conformation, due to the difference in the hydrodynamic drag force exerted by the fluid on a coiled polymer compared to a stretched polymer.⁸⁵ Specifically, at intermediate $Wi_e \approx 0.5$, the drag force on a coiled polymer is insufficient to extend it, but is large enough to maintain the extension of an initially stretched polymer. This difference in hydrodynamic drag creates a hysteretic dependence of polymer extension on strain history: with increasing Wi_e , polymer stretching occurs at $Wi_{e,stretch} \approx 0.6$, while with decreasing Wi_e , coiling occurs at a lower $Wi_{e,coil} \approx 0.4$ (Figure 4). This hysteresis is a signature of a discontinuous first-order transition as

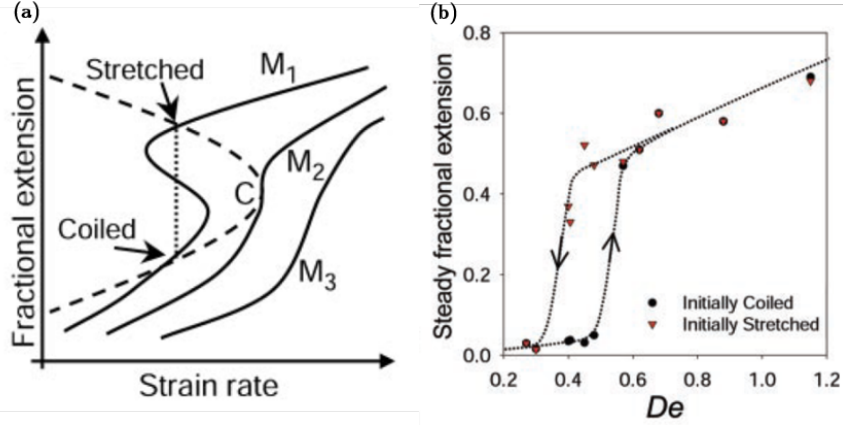


Figure 4: (a) Sketch of hypothesized coil-stretch hysteresis for higher molecular weight polymers ($M_1 > M_2 > M_3$), drawing an analogy to the liquid-vapor binodal in the style of de Gennes.^{85, 107} (b) Equilibrium conformations of DNA from direct observation in a microfluidic cross-slot trap show a hysteresis window about $Wi_e \sim 0.4 \pm 0.1$ (termed De here), consistent with the hypothesized hysteresis window in (a).⁸⁵ Copyright 2003, AAAS; reprinted with permission.

theoretically predicted,¹⁰⁷ and thus both coiled and stretched polymers can coexist for $Wi_e \approx 0.5 \pm 0.1$. This bistability in conformations and coil-stretch hysteresis manifests in a broad range of conditions, including in the unstable flows described in §5.¹¹²

In flows with intermediate to high Deborah numbers $De \gtrsim 1$, the polymer chains do not have adequate time to reach these equilibrium conformations—instead, transient elongation and relaxation dynamics dominate.^{113–115} Microfluidic measurements of transient single-polymer relaxation have provided scaling relationships for polymer relaxation and retardation times, which change in the dilute and semi-dilute regimes.^{116, 117} Moreover, in startup flows, polymers can overshoot their equilibrium conformations before relaxing¹¹⁸—even becoming kinetically trapped in kinked or knotted conformations. These kinks and knots can strongly increase the rate of polymer elongation, and hence the ‘retardation time’ needed by the chain to reach equilibrium.⁹⁵ Direct visualization of dilute DNA reveals four dominant conformations during transient elongation: dumbbell, kinked, half-dumbbell, and folded (Figure 5).¹⁰² For more concentrated semi-dilute solutions, interactions with other chains also influence the kinetics of stretching;¹¹⁷ for example, kinks and folds are typically suppressed, and chains can instead have coiled ends, which again increase the polymer retardation time. Thus, for startup or highly time-dependent flows, kinetic trapping of polymers can lead to many more unique conformations, which may influence bulk flow properties.

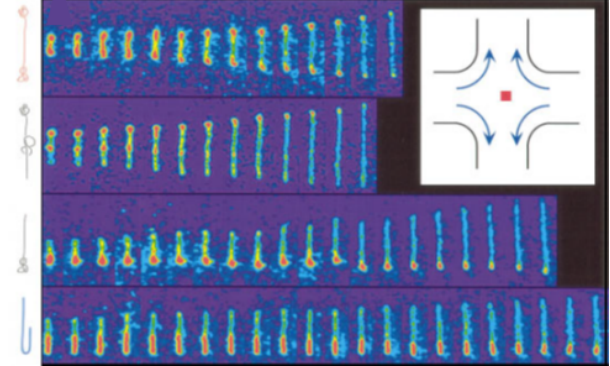


Figure 5: Kinetically trapped conformations of DNA in an extensional trap after rapid startup flow show several different transient conformations based on initial conditions: dumbbell, kinked, half-dumbbell, and folded (top to bottom).¹⁰² Copyright 1997, AAAS; reprinted with permission.

Direct visualization using microfluidics confirms that polymer chains are abruptly elongated as they transit through a microfluidic pore space. Individual polymers flowing around channel-centered cylindrical obstacles are highly stretched (Figure 6a-c), producing excess flow resistance consistent with the abrupt increase of η_{app} in bulk porous media.¹⁰⁵ These elongated chains in turn align at a sudden contraction to form large vortices (Figure 6d).¹⁰¹ The mechanism for eddy formation is similar to the case of rigid polymers (§4.1): eddy formation minimizes the extensional stress penalty of misaligned chains.

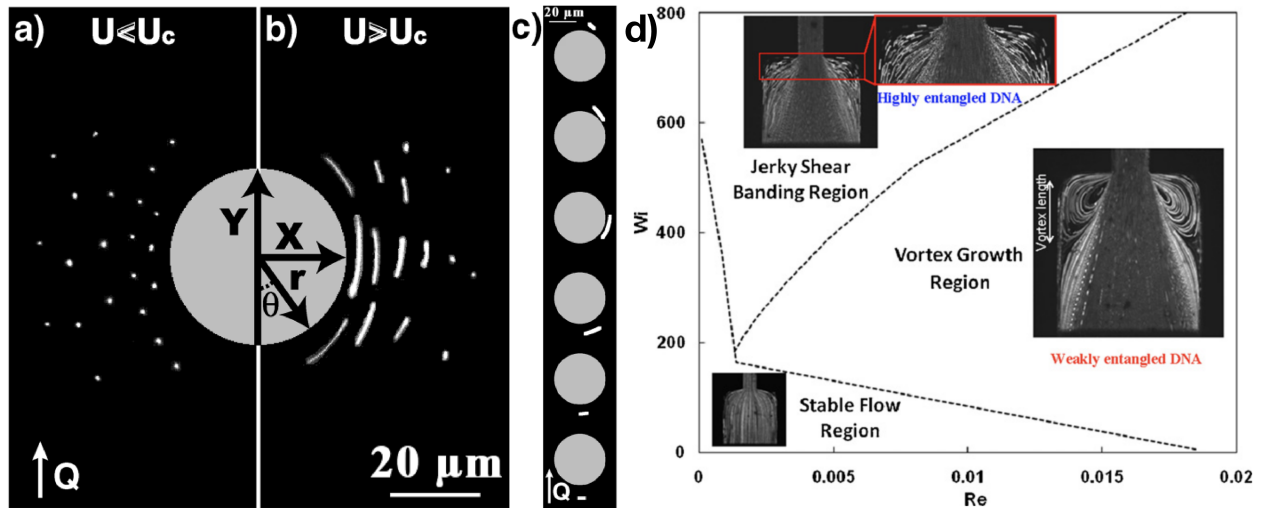


Figure 6: (a-c) Fluorescent micrographs of labeled DNA molecules flowing around a cylinder in a microfluidic channel (flow is bottom to top) at (a) a low flow rate below the coil-stretch transition, or at (b) a high flow rate above the coil-stretch transition. The chain elongation is strongest closest to the cylinder. (c) A sequence of images showing the DNA molecule approaching the cylinder and elongating when it is sufficiently close.¹⁰⁵ Copyright 2008, American Physical Society; reprinted with permission. (d) Streakline images of fluorescent tracer particles shows the generation of large vortices at the entrance of a sudden contraction. Visualization of fluorescently labeled DNA confirms that DNA elongation drives the eddy growth. For highly entangled solutions, the eddies show transient fluctuations.¹⁰¹ Copyright 2010, Elsevier; reprinted with permission.

Notably, these polymer chain conformations are highly time-dependent, leading to transient flow effects.^{113–115} For example, in the simple case of a sudden constriction, the dynamic stretching and coiling of highly entangled polymers can produce time-dependent shear-banding and eddies with fluctuating surfaces (Figures 2 and 6d).^{52,101} In micromodels with a channel-centered cylinder, transient polymer extension can lead to a time-dependent macroscopic flow resistance.^{105,106} Hence, the extensional viscosity η_e only quantifies the elongation contribution to fluid stress when averaged over sufficiently large spatial and temporal scales. Recent work has also demonstrated the strong role of polymer elongation on the breakup dynamics of aqueous droplets, indicating that such transient extension likely plays an important role in flows involving fluid interfaces, as in EOR and groundwater remediation.^{67–69} While these transient effects have typically been neglected in models of polymer solution flow through porous media, ongoing work leveraging microfluidics is beginning to shed light on the central influence of unsteady flows in determining macroscopic transport properties. We thus turn our attention to these time-dependent behaviors in the next Section.

5 Unstable Flow of Polymer Solutions

5.1 Unstable Flow of Bulk Solutions

In a heterogeneous porous medium, Wi is determined by the deformation of the polymers near the curved solid surfaces, and so depends on the local fluid deformation rate. Alternatively, De depends on the time needed for the polymers to traverse each individual pore. Thus, when both Wi and De are $\gtrsim 1$, chain elongation cannot keep up with the changing flow field as a polymer transits through the pore space, leading to the development of an unsteady flow state with continual fluctuations in polymer conformation—further described in §5.2.

A similar instability can arise in bulk solution if the polymer chains are forced to flow along highly-curved fluid streamlines; fluctuations in the polymer conformations build up elastic stresses in the solution, leading to sustained spatial and temporal flow fluctuations reminiscent of ‘conventional’ turbulence, which arises at $Re \gg 1$. In the inertial case, turbulence arises because the non-linear inertial term in the Navier-Stokes equations destabilizes the steady-state laminar solution. Similarly, in the inertia-free case of polymer solutions at $Re \ll 1$, a flow instability analogous to turbulence arises because non-linearities in the constitutive relation between stress and deformation (§3.2) destabilize the steady-state laminar solution. Such instabilities were theorized as early as the 1970s^{21,119} and have been catalogued in diverse geometries, including concentric cylinders, rotating disks, and curved channels since the late 1980s.^{22,120–146} In all cases, an instability is observed for strong enough flow in geometries with a large amount of streamline curvature.

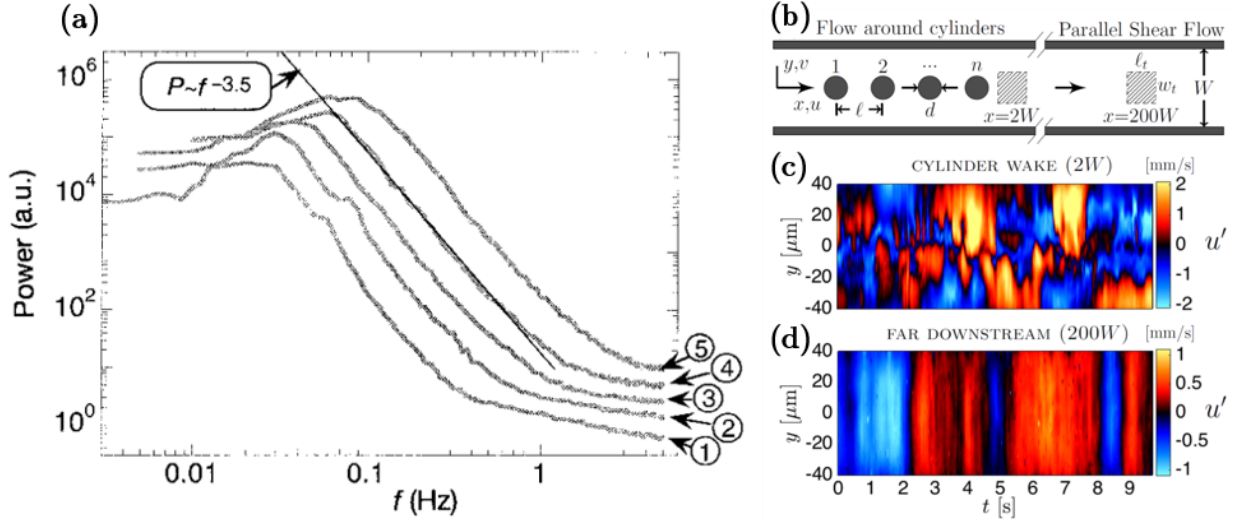


Figure 7: **a** Power spectra of velocity fluctuations for applied shear rates ($\dot{\gamma} = 1.25, 1.85, 2.7, 4$, and 5.9 s^{-1} for lines 1–5 respectively) in a cone-plate rheometer.²³ Copyright 2000, Springer Nature; reprinted with permission. **b** Schematic of microfluidic porous media, and kymographs of streamwise velocity fluctuations (u') nearby (c) and far downstream (d) of circular pillar array.¹⁴⁷ Copyright 2017, American Physical Society; reprinted with permission.

Groisman and Steinberg gave strong quantitative evidence that this flow instability, even though it arises for $Re \ll 1$, shares many features with high- Re inertial turbulence—hence, this unsteady flow behavior is often termed ‘elastic turbulence’.²³ In particular, they showed

that the power spectrum of the velocity fluctuations of a polymer solution, sheared at a sufficiently large rate in a cone-plate rheometer, decays as a power law in spatial and temporal frequency (Figure 7 a). Thus, the fluid motion is excited over a broad range of spatial and temporal scales, similar to high-Re turbulence; intriguingly, however, this power law decay (with a -3.5 exponent) has a different value than the -5/3 Kolmogorov exponent characteristic of high-Re turbulence. Simulations are able to recover a similar spectral scaling, supporting the idea that it reflects an elastic instability analogous to turbulence;^{148,149} they also reveal that flow fluctuations are stronger near boundaries,¹⁴⁹ potentially due to a depletion layer effect.¹⁵⁰

Single-molecule imaging of fluorescently-labeled DNA demonstrates that a sharp coil-stretch transition occurs in these unstable flows.¹¹² In this case, the mean elongation for polymers in the ‘stretched’ state is found to be approximately 0.85 the contour length.^{151,152} Thus, the development of an unstable flow state characterized by sustained flow fluctuations is thought to be linked to the continual elongation of polymer chains. Flow birefringence and single-molecule imaging confirm this expectation. In particular, they demonstrate that flow fluctuations are indeed linked to the continual elongation of polymer chains, which arises for sufficiently large Wi .^{125,153–156} This picture is further supported by the finding that polymers with more backbone rigidity have suppressed fluctuations, demonstrating that polymer chain stretching is indeed required for this instability.¹⁵⁷

Studies of this instability in microfluidic channels shed additional light on its spatial dependence. For example, measurements in a linear channel with straight walls demonstrate that the unstable flow state arises when the fluid is sufficiently perturbed through collisions with an array of pillars. Once sufficiently perturbed, the flow remains unsteady far downstream of the perturbation; this observation suggests the generation of a new dynamical flow state in which fluctuations are sustained indefinitely.¹⁵⁸ However, the statistics of the flow fluctuations are markedly different near the pillars and far downstream.¹⁴⁷ As the flow progresses downstream, regions of positive or negative streamwise velocity fluctuations coalesce, leading to large rolling advection cell structures (Figure 7 b–d). Moreover, the velocity power spectra show different power-law decays, with a -1.7 exponent near the pillar array and a -2.7 exponent far downstream. These different spectra are concomitant with spatial differences in the measured variation of the shearing and elongational components of the velocity gradient, which mediate polymer stretching. In particular, as the flow progresses downstream, the variation in the elongational component of the velocity gradient dominates, suggesting that the polymer molecules are increasingly stretched by flow gradient in the streamwise direction. These results provide evidence that the unstable state of ‘elastic turbulence’ can develop spatially in parallel channels, suggesting a strong dependence on system geometry.

In most geometries, the base laminar flow field is characterized by a complex interplay between shear and extension; thus, even predicting the onset of unstable flow can be challenging. Intuitively, one expects that it arises when elastic stresses—characterized by a large value of $Wi \equiv N_1(\dot{\gamma})/2\sigma(\dot{\gamma})$ —persist over a chain relaxation length scale λU exceeding the effective streamline radius of curvature \mathcal{R} . This effective curvature can be thought of as the length scale over which the fluid perturbation persists; thus, the ratio $\lambda U/\mathcal{R}$ is equivalent to the Deborah number De . Thus, one expects that unstable flow arises when the product $Wi \cdot De$ is sufficiently large,¹⁵⁹ as found in early experimental work.^{21,22} A linear stability analysis of the Upper Convected Maxwell model quantifies this expectation, showing that

the largest destabilizing term in the Navier-Stokes equations is of order

$$M \equiv \left(\frac{N_1(\dot{\gamma})}{\sigma(\dot{\gamma})} \frac{\lambda U}{\mathcal{R}} \right)^{1/2}$$

where in practice, the effective radius \mathcal{R} corresponds to the smallest streamline radius of curvature that elongates polymer chains. This quantity can thus be an order of magnitude smaller than the other characteristic length scales in a given flow geometry,¹⁶⁰ but nevertheless can be empirically calculated from the structural parameters of the system.¹²⁵ Unstable flow is thus predicted to arise above a threshold value of this universal parameter, typically called the M parameter, as defined using the expression above by Pakdel and McKinley in 1996.¹⁵⁹ This expectation was confirmed experimentally for diverse flow geometries;^{125, 161, 162} in practice, the threshold M ranges between ≈ 6 and 12 in different geometries, and determining exactly why this threshold value varies between experiments is still a topic of current research. Importantly, polymer solutions applied in EOR and groundwater remediation can have M ranging from $\sim 10^{-6}$ to 10^6 , indicating that unstable flow can arise in many of these cases.

5.2 Unstable Flow in Microfluidic Porous Media

Does unstable flow persist in a porous medium? And if so, how does the interplay between unstable flow and pore space geometry impact the flow field and macroscopic flow resistance? Microfluidic investigations over the past two decades have played—and continue to play—a critical role in addressing these questions. Both experiments and complementary simulations have focused on pore space geometries that vary in complexity, ranging from a single contraction, to a single flow obstacle, to a linear channel of obstacles, to a 2D lattice of obstacles, all of which enrich our understanding of unstable flow in porous media. Indeed, unstable flow is expected to arise when high-molecular weight polymers are injected at large speeds; under these conditions, the polymers cannot equilibrate to the continually-changing stresses as they are advected through the tortuous pore space.

The simplest model of a pore is a single abrupt constriction. As it enters the constriction, a flowing polymer solution forms large upstream eddies above a threshold value of M . While reminiscent of the steady eddies formed by rigid and elongated polymers (§4.1 and §4.2), these eddies fluctuate strongly in time.¹⁶⁵ The eddy size and asymmetry increases nonlinearly with Wi and with increasing contraction ratio β , as summarized in the state diagram shown in Figure 8a.^{155, 163, 166–168} In one study,¹⁶⁹ the eddy length L_e was measured to grow as $L_e/W \sim Wi^{0.45}$, where W is the channel width upstream of the constriction, but a universal scaling has not been established. However, similar flow structures can be replicated in simulations,¹⁷⁰ suggesting that eddy formation is more general. Interestingly, the presence of inertia suppresses temporal fluctuations of these eddies, and promotes symmetry in their structure (Figure 8b).^{48, 164}

Flow through a pore is often represented instead by flow impinging on a channel-centered cylinder. Single-molecule imaging of fluorescently-labeled DNA provides evidence that polymers are stretched and have hysteretic conformations as they flow around the cylinder¹⁰⁶ in a manner similar to coil-stretch hysteresis (§4.2). Thus, similar to the case of flow through

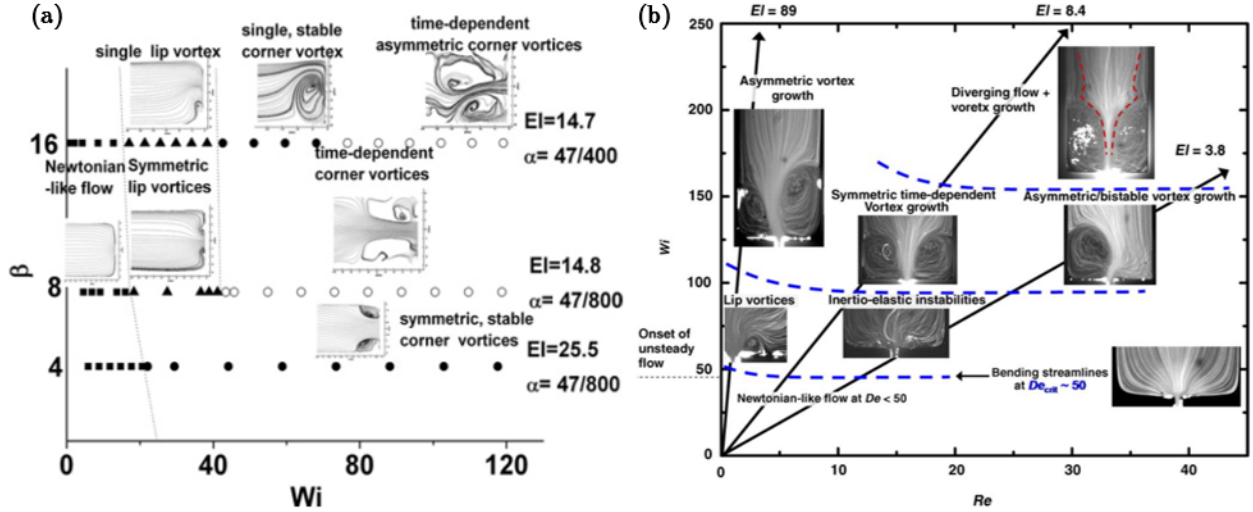


Figure 8: State diagrams indicating the structure of unstable eddies upstream of a sudden constriction at different elasticity numbers, $El \equiv Wi/Re$, and at different constriction ratios α , defined as the ratio between the constriction width and the expansion width. **a** Role of constriction ratio β and Wi .¹⁶³ Copyright 2011, Elsevier; reprinted with permission. **b** Role of Re and Wi .¹⁶⁴ Copyright 2005, Elsevier; reprinted with permission.

a constriction, upstream eddies form during polymer solution flow around a cylinder in a narrow channel, growing in size and becoming unstable as Wi increases.¹⁷¹ Holographic imaging enables full characterization of the complex 3D structure of these eddies (Figure 9). Intriguingly, the vertical location of the eddy can exhibit discrete switching between the top and bottom walls of the channel,¹⁷¹ suggesting a possible connection to bistable polymer conformations (described in the context of the coil-stretch transition in §4.2). Exploring this connection will be a valuable direction for future work. Eddy formation is not general to all such flows: for example, eddies are not observed for polymer solution flows impinging on a cylinder in a wide channel. Instead, an extended wake forms downstream in which the extended chains gradually relax to their equilibrium conformations.^{145,146,173}

Real-world porous media are typically composed of many interconnected pore expansions and contractions. To more closely mimic this geometry, experiments have investigated polymer solutions flowing through channels with multiple constrictions, channel-centered pillars, and undulating walls arranged in 1D or in 2D arrays. Results obtained for ordered 1D arrays of pores in channels of narrow widths consistently demonstrate the formation of unstable eddies upstream of constrictions, similar to the case of a single constriction (Figure 10a-h);^{123,174,175} these eddies also form in flows with moderate inertia ($Re \sim 20$).^{49,176,177} Unstable eddies similarly form in the simple case of a channel with two channel-centered cylinders.¹⁷² However, when the channel width is made larger, eddies are not observed; instead, an extended wake forms downstream of each cylinder, similar to the case of a single cylinder in a wide channel.¹⁷³

Because polymer stretching is hysteretic and can persist over large length scales,¹⁴⁷ polymer elongation may be retained across multiple pores. This ‘memory’ may therefore provide new spatial structure to the flow over macroscopic scales in a porous medium. Studies of ordered 1D arrays are beginning to reveal such effects. For example, decreasing the distance

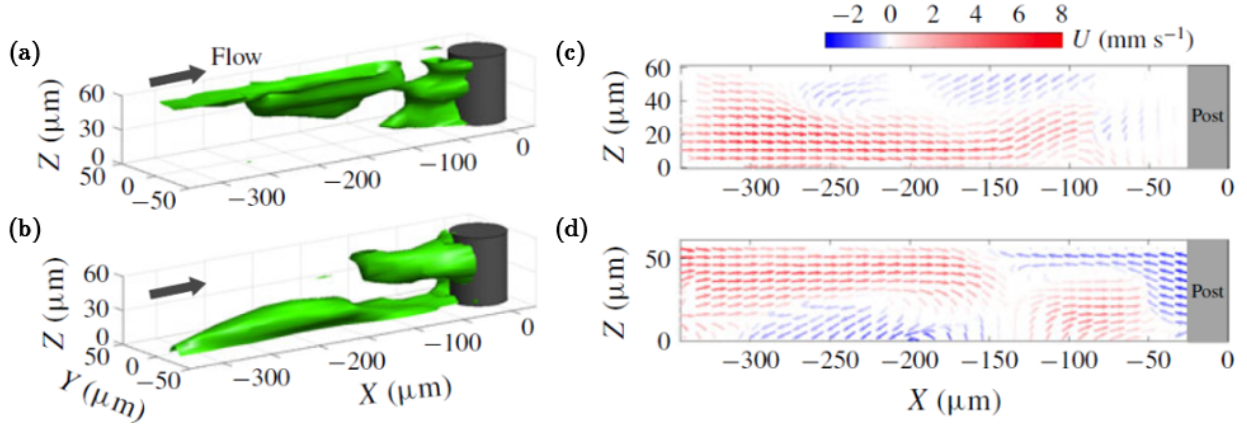


Figure 9: Unstable eddy upstream of a single channel-centered cylinder. The vertical location of the eddy switches between the top and bottom walls over time.¹⁷¹ Copyright 2019, Cambridge University Press; reprinted with permission.

between pillars in a narrow channel produces stronger fluctuations at similar values of Wi ;¹⁷⁷ conversely, in a wider channel, the wake formed downstream of a first cylinder can merge with the wake formed downstream of a second.¹⁷³

This complex coupling between pores also manifests in 2D arrays, showing flow behavior that can differ strongly from the 1D case. For example, polymer solutions flowing through ordered 2D arrays show strong velocity fluctuations throughout the pore space—but eddies are never observed.^{14,74} Intriguingly, in other studies of flow through ordered 2D arrays of circular, square, and triangular pillars, large triangular ‘dead zones’ form on the upstream faces of the pillars; these dead zones are characterized by strong polymer compression and elongation, but unlike eddies, they show no apparent recirculation.^{50,178} These dead zones periodically grow and disappear; moreover, the frequency of this process increases further downstream along the porous medium, indicating that coupling between pores influences the flow.⁶⁰ Consistent with these observations, the temporal variation in pressure measurements increases downstream along ordered 2D arrays of circular pillars, suggesting that instabilities grow spatially.^{98,174}

Combining such flow visualization to measurements of the overall pressure drop provides a way to directly link flow structure to macroscopic flow resistance. Such measurements show a dramatic increase in macroscopic flow resistance—mimicking the increase in η_{app} observed in bulk porous media—at the onset of unstable flow (Figure 10i).^{14,172,179,180} Simulations in model porous geometries can also capture the onset of flow fluctuations^{181–183} and the associated increase in flow resistance.^{184–186} These recent findings thus suggest the possibility that the striking increase in polymer solution flow resistance measured in bulk porous media reflects the onset of unstable flow.

Real-world porous media, however, are typically disordered: the pore sizes and spacing between grains are not uniform. While the majority of experiments and simulations have focused on studying polymer solution flow in ordered arrays, ongoing work is beginning to reveal that structural disorder can dramatically impact flow behavior. For example, flow visualization in 2D arrays of circular pillars shows that while a highly unstable flow state arises in an ordered medium due to sustained polymer elongation, velocity fluctuations are nearly

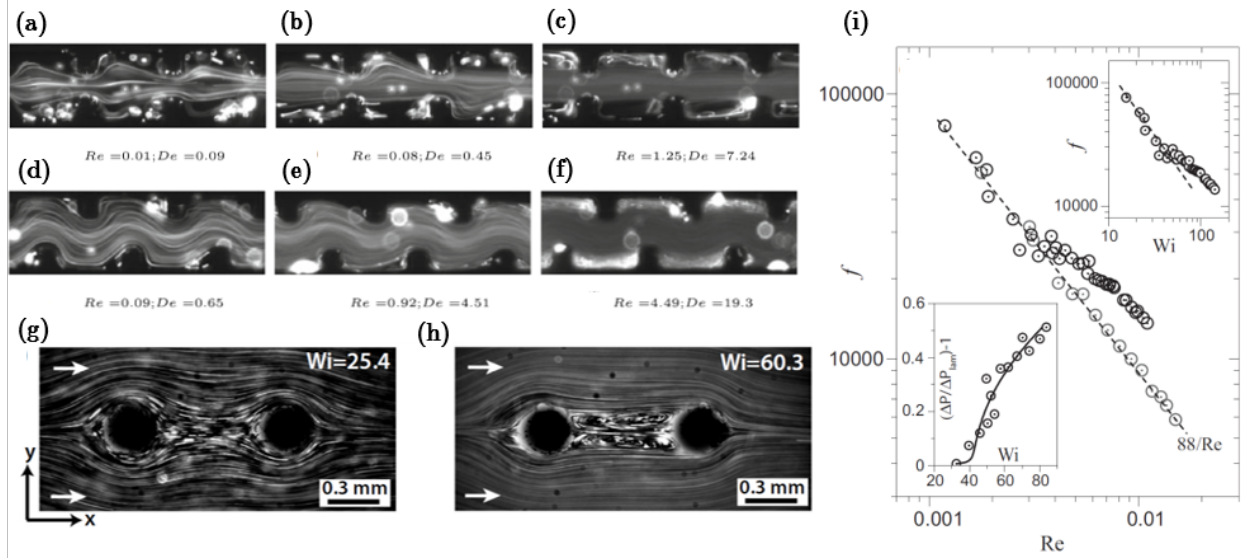


Figure 10: (a-h) Flow structures of unstable polymer solution flow in a channel of square contractions, offset square contractions,¹²³ and channel-centered cylinders.¹⁷² Copyright 2012, Springer; reprinted with permission. (i) Plot of the flow friction factor $f \equiv 2D_h \Delta P / \rho U^2 L$, which quantifies flow resistance, for the overall microfluidic channel in the experiment shown in (g-h); D_h is the hydraulic radius of the channel, ΔP is the pressure drop measured over the total length L , ρ is the fluid density, and U is the average channel flow speed. Light grey circles are for a Newtonian fluid while solid black circles are for a solution of 18 MDa polyacrylamide at 100 ppm, corresponding to half the overlap concentration C^* . The friction factor departs from the expected Newtonian trend (dashed line) despite the low Re . Insets show that this sudden increase in the flow resistance occurs above a critical Wi corresponding to the onset of the flow instability observed in panels g and h.¹⁷² Copyright 2017, American Physical Society; reprinted with permission.

completely suppressed in a disordered array.¹⁸⁷ Analysis of the pore-scale velocity field suggests an explanation: in a disordered array, interactions between the pores causes the flow to concentrate in finger-like channels dominated by shear, not elongation (Figure 11). This suppression of elongation can be interpreted as a local reduction in $Wi \equiv N_1 (\dot{\gamma}) / 2\sigma (\dot{\gamma})$, and thus a local reduction in M , which quantifies flow destabilization. Other 2D experiments indicate a key influence of polymer solution rheology on the formation of these finger-like channels, suggesting that they develop when the fluid is shear-thinning and thus can flow more easily in channels of high shear. Hence, while microfluidic experiments in ordered arrays suggest a tantalizing link between the onset of unstable flow and the increased flow resistance measured in bulk porous media, the influence of pore-scale disorder and fluid rheology complicate this interpretation. Developing a unified understanding of unstable polymer solution flow through porous media—which would enable accurate prediction of the pore-scale flow structure and macroscopic transport behavior—therefore remains an important and outstanding goal for future work.

6 Improved Fluid Recovery From Porous Media

A prominent application of polymer solutions is to recover trapped non-aqueous fluid from porous media in EOR and groundwater remediation. In these cases, globules of oil or an

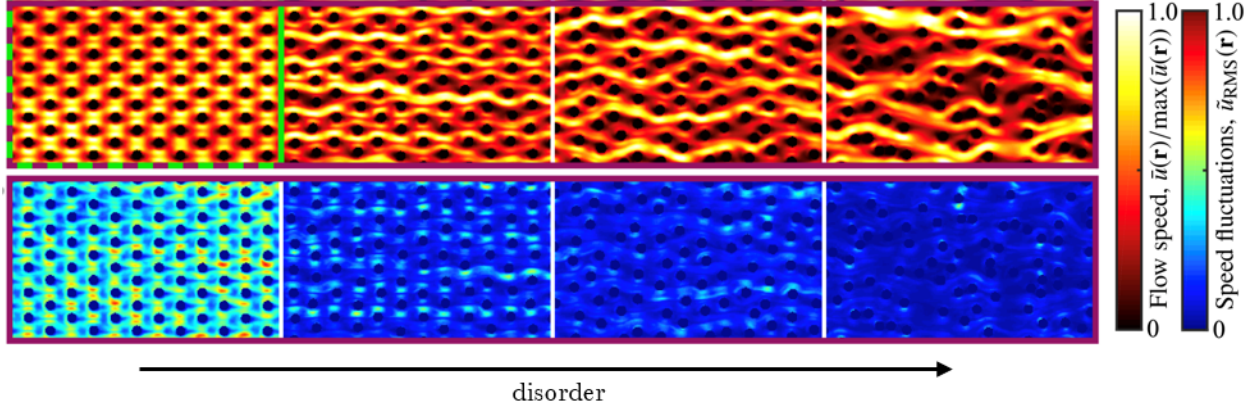


Figure 11: Top row shows normalized time-averaged speed field for $Wi \approx 4$. Bottom row shows corresponding normalized map of speed fluctuations. Left-most column is a perfectly-ordered array, characterized by strong fluctuations; disorder increases moving to the right, showing that disorder promotes the formation of preferential flow channels and suppresses flow fluctuations.¹⁸⁷

organic contaminant are trapped in the pore space by capillary forces. A globule of length L_{glob} along the flow direction can only be displaced out of the pores when the viscous pressure drop across it, $|\Delta P| = \eta_{\text{app}}(Q/A)L_{\text{glob}}/k$, exceeds the capillary pressure threshold $\sim \gamma/a$ for squeezing the fluid-fluid interface through the pores, where γ is the interfacial tension and a is the pore size.¹⁸⁸ This criterion is often expressed in terms of the Capillary number, $Ca \equiv \eta_{\text{app}}(Q/A)/\gamma$; displacing trapped non-aqueous fluid globules usually requires $Ca \geq 10^{-4}$, which is higher than is typically accessible in field applications (Table 2).^{188–190}

Conventional belief has held that polymer solutions are not able to increase Ca far above this threshold under typical operating conditions. As a result, dilute solutions of low molecular weight polymers have traditionally been used simply to suppress fingering instabilities during injection and thereby maintain flow uniformity during fluid recovery.^{1,15} However, this view has recently been challenged: EOR field tests with more concentrated solutions of high molecular weight polymers often yield unexpectedly high recoveries of oil fluid far beyond what is expected from a simple estimate of Ca with η_{app} given by the shear viscosity.^{9–13,191} These findings have prompted the use of concentrated polymer solutions for groundwater remediation as well.^{2,89,192,193}

Unfortunately, inconsistencies in the literature make it difficult to define the conditions for improved fluid displacement: many studies report improved oil recovery from sand packs and cores when polymer solutions are injected,^{10,13,20,194} while others report no change or decreased recovery compared to polymer-free water.^{192,195,196} Reconciling these inconsistencies is challenging, due to the inability of typical experiments to probe the flow behavior inside the pore space with sufficient spatial and temporal resolution. As a result, the mechanisms by which polymer solutions can enhance fluid recovery remain poorly understood and hotly debated.^{40–42} Hence, microfluidic platforms are increasingly being used to shed light on fluid displacement from porous media.^{9,51,197,198}

Several proposed mechanisms rely on a potential influence of polymers on the immiscible fluid interface. For example, it has been speculated that polymer solution viscoelasticity alters the shape of the fluid displacement front in a porous medium.¹⁹⁹ However, how this

process impacts macroscopic fluid recovery is unclear. In another mechanism, it is speculated that the extensional viscosity of polymer solutions suppresses non-aqueous globules from breaking up as they transit through the tortuous pore space. This breakup process—analogue to the Rayleigh-Plateau instability—is thought to arise in strongly disordered pore geometries²⁰⁰ and results in globules with smaller L_{glob} . The viscous pressure drop across each globule, and thus its ability to be displaced and recovered, is thus reduced. Due to their extensional viscosity, polymers are thought to suppress this breakup process—as shown in idealized experiments and simulations^{201–204}—and thereby improve non-aqueous fluid recovery. Experiments on bulk rock cores show indirect agreement.²⁰ However, direct confirmation of this effect inside a porous medium, and quantification of the potential increase in fluid recovery, is lacking. Addressing these questions will be a valuable direction for future work.

Other proposed mechanisms rely on an increase in η_{app} , which therefore increases Ca, potentially above the threshold needed to displace trapped non-aqueous fluid globules. This view is supported by measurements on bulk porous media that directly link an increase in macroscopic flow resistance to enhanced fluid recovery.^{9–14}

As described in §4.1, one possibility is that polymer adsorption onto the solid matrix partially or fully clogs pores and increases η_{app} .^{18,19,89} While experiments suggest that this mechanism is frequently present, the resultant increase in local flow resistance is often much smaller than the measured macroscopic increase in η_{app} , and thus cannot fully explain enhanced fluid recovery.⁹⁰

As described in §3.1, another possibility is that the measured increase in η_{app} reflects an increase in the polymer extensional viscosity. Microfluidic platforms provide a way to directly quantify this effect, revealing that for sufficient extension rates, the extensional viscosity can indeed abruptly increase⁷⁰—potentially providing a sufficient increase in η_{app} to displace trapped fluids.^{16,17} However, quantitative tests of this idea are limited, and future work is needed to determine if the expected increase of η_{app} results in a sufficient increase in Ca to enhance fluid recovery.

Recent work suggests a key role played by flow instabilities in enhancing fluid recovery. Indeed, microfluidic experiments have shown that unstable flow is often characterized by a dramatic increase in η_{app} , as described in §5.2—leading to a concomitant increase in Ca.^{14,172,180,186,206} This idea has been directly verified using oil globules trapped in a microfluidic porous medium: injecting polymer solutions can increase the apparent Ca by nearly an order of magnitude, thereby increasing oil recovery (Figure 12a-b).⁵¹ Independent measurements on different microfluidic porous media show similar results, and demonstrate that the increase in Ca coincides with an abrupt increase in flow fluctuations, reflecting the onset of unstable flow.¹⁴ In addition to increasing η_{app} , imaging suggests that these flow fluctuations can also induce fluctuations at the aqueous/non-aqueous fluid contact line with the solid matrix (Figure 12d). These fluctuations are speculated to reduce contact line pinning, thereby further promoting trapped globule displacement.^{14,25} Together, these results provide compelling evidence that flow instabilities can in some cases contribute to the increase in macroscopic flow resistance, and the concomitant increase in non-aqueous fluid recovery, that has been observed in bulk porous media. Careful assessment of the generality of this phenomenon, and developing the ability to predict the magnitude of increased flow resistance and fluid recovery, will therefore be an important direction for future research.

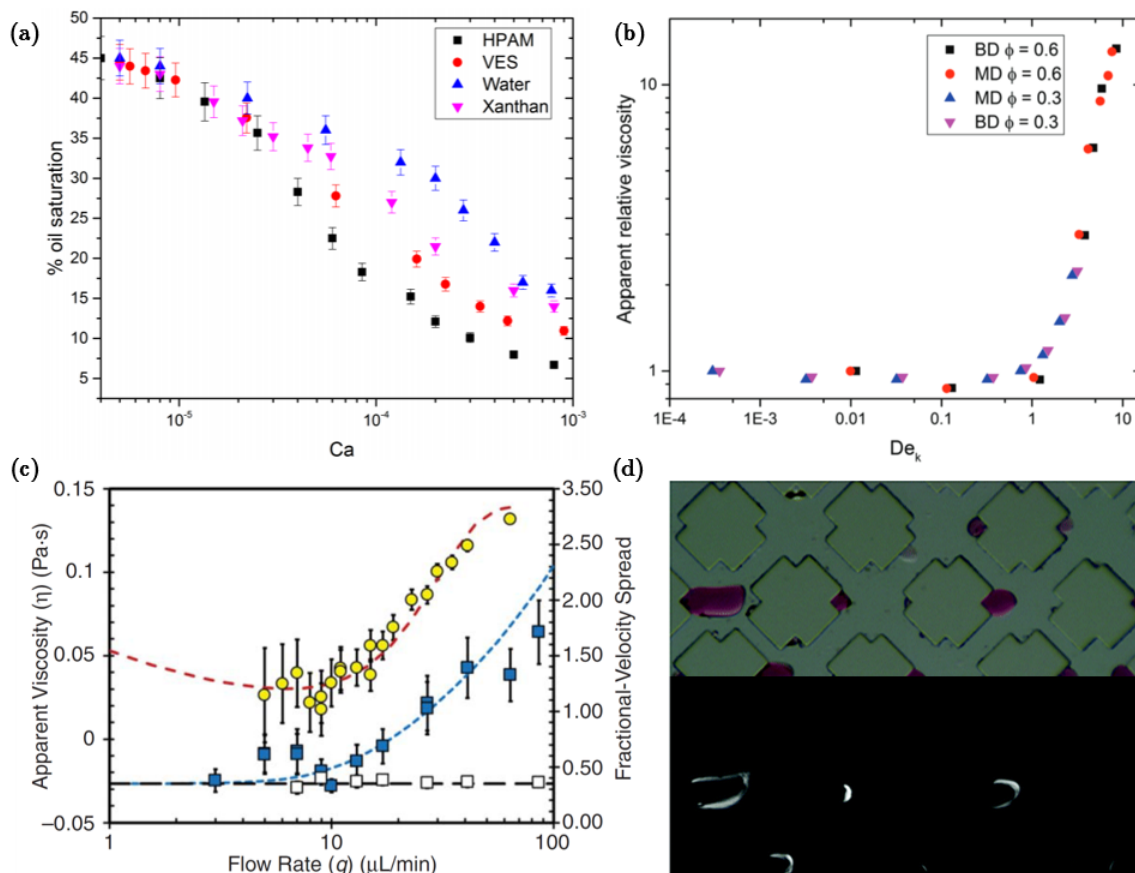


Figure 12: **a** Reduction in oil saturation at similar apparent capillary numbers Ca by introducing polymers.¹⁸⁰ Copyright 2018, Elsevier; reprinted with permission. **b** Simulations qualitatively match the experimental increase in flow resistance (η_{app}) at the onset of unstable velocity fluctuations.¹⁸⁶ Copyright 2017, Royal Society of Chemistry; reprinted with permission. **c** Apparent thickening of η_{app} (circles) coincides with increased velocity spread for polymer solution flow (filled squares) over Newtonian baseline (open squares).²⁰⁵ **d** The onset of velocity fluctuations and the increase in flow resistance is also coincident with observed fluctuations in the aqueous-nonaqueous interfaces, and an improved displacement of oil globules. Top shows image of oil trapped in microfluidic porous network; bottom shows integrated difference images, which indicate interface fluctuations.²⁰⁵ Copyright 2015, Royal Society of Chemistry; reprinted with permission.

7 Outlook

We have described how, through precise control over channel geometry, flow conditions, and simultaneous flow visualization, microfluidic technologies shed light on the unusual flow properties of polymer solutions in porous media. Specifically, microfluidic experiments have deepened our understanding of how single-molecule elongation increases steady-state flow resistance and generates an unstable flow state. Together, these effects help to explain macroscopic measurements of increased flow resistance and fluid recovery from bulk porous media. Thus, by providing a fundamental understanding of the underlying physics, these studies help to provide quantitative principles by which polymer solution flows can be predicted and controlled for applications like enhanced oil recovery and groundwater remediation. However, several key questions remain unanswered, which we highlight below as possible directions for

future research in this area.

Extensional viscosity measurements. Microfluidic devices with precisely-controlled boundaries now enable the investigation of flows with pure extension, as described in §3.1. Such platforms provide an opportunity to systematically measure extensional viscosity over different extension rates. While shear viscosity measurements abound, many applications involve the use of polymer solutions under extension. Obtaining measurements of extensional viscosity for different classes of polymers, in different solvents and environmental conditions, will provide key data to guide these applications. Moreover, these data will enable quantitative assessment of the contribution made by extensional viscosity to macroscopic flow resistance measured for bulk porous media.

Contribution of eddies to flow resistance. As described in §4.1, eddies often form when polymer solutions are forced through constrictions. These regions of intense recirculation pose an additional source of dissipation and thus contribute to the macroscopic pressure drop. However, a way to quantitatively predict the contribution of eddies to macroscopic flow resistance is lacking. Systematic tests of eddies formed using polymers of different flexibilities and molecular weights could provide crucial data that could help address this gap in knowledge.

Transient molecular conformations. While imaging of single molecules in microfluidic channels (§4.2) reveals that hysteretic and transient conformations (e.g. dumbbell, kinked, half-dumbbell, folded, end-coiled) impact chain relaxation dynamics, it is unclear whether such transient states arise in flow through more complex porous media, and whether they influence flow behavior. Single-molecule imaging of large polymers in model porous media could provide an answer.

Confinement effects. In highly-confined pore spaces, polymer repulsion from the walls can create a depletion layer.^{207,208} This depletion layer arises from a combination of shear-induced migration,^{209–211} entropic or steric effects,²¹² and electrostatic interactions.²¹³ Though typically neglected from macroscopic models of flow, the formation of a depletion layer could play a considerable role on transport—for example, possibly suppressing polymer adsorption and leading to viscosity reduction at the pore surfaces.¹⁵⁰ Nanofluidic platforms, which provide a means to test pores of width approaching molecular dimensions, could shed light on these effects.

Universal description of unstable flow. While the onset of unstable flow can be predicted for polymer solutions in bulk media (§5.1), how to generally predict this onset in heterogeneous porous media is unknown. The M parameter that universally predicts instability in bulk flows incorporates the effective streamline curvature \mathcal{R} ; however, it is unclear how to calculate \mathcal{R} to accurately describe a highly tortuous pore space.

Most experiments are reported in terms of the Weissenberg number Wi , and often use the approximate form $Wi \equiv \lambda \dot{\gamma}$, with differing choices of λ and how to calculate $\dot{\gamma}$. As a result, a wide range of different flow behaviors is reported. Moreover, while recent experiments suggest that unstable flow can develop spatially due to coupling between flow in different pores, an understanding of this behavior is lacking. An open challenge is to develop a unified description of these diverse flow behaviors, capable of predicting the unstable flow that arises for different polymer solutions, pore space geometries, and imposed flow conditions.

Different fluid displacement mechanisms. As described in §6, numerous mechanisms have been identified to explain how polymer solutions can enhance recovery of trapped non-

aqueous fluid from porous media. However, quantitative and predictive models of fluid recovery remain lacking. Studies typically focus on describing one mechanism, while in reality multiple mechanisms may be at play—thus hindering a unified understanding of fluid recovery. Thus, an important direction for future work will be to systematically assess the occurrence and relative influence of the different mechanisms identified thus far (suppressed fluid break up, permeability reduction through polymer adsorption, the contribution of extensional viscosity, enhanced dissipation and contact line fluctuations due to unstable flow) under different flow conditions.

Pore-scale disorder. While the majority of experiments and simulations have focused on studying polymer solution flow in ordered arrays, real-world porous media are typically disordered. Recent work has shown that disorder may strongly alter flow behavior—in some cases, completely suppressing the onset of unstable flow. However, predicting when this suppression arises—i.e. how sensitive it is to the pore-space geometry—and why it arises is still an open challenge.

Microfluidic surface chemistry. Most microfluidic visualization studies use devices made with PDMS, which may not adequately recapitulate the complex surface chemistry of real-world porous media. However, advances continue to be made in the development of microfluidic channels etched directly into mineral substrates, thus enabling flow visualization in channels with surfaces made of real rock material.^{214–217} While this technology has been used to shed light on questions relating to chemical reactions in porous media, it has yet to be employed in studies of polymer solution flow.

Fluid rheology. While some simulations suggest that shear-thinning effects do not influence polymer solution flow, other work suggests a dominant role for the fluid shear rheology. For example, shear-thinning is speculated to promote the formation of preferential flow channels, which reduce polymer elongation. Thus, developing a quantitative description of how fluid rheology impacts the flow behaviors described in this paper is an important direction for future work.

Pore space dimensionality. The pore space of a 2D medium is considerably less connected and tortuous than that of a disordered 3D medium. This difference can lead to dramatic differences in polymer solution flow behavior and fluid recovery; thus, the applicability of experiments performed on 2D microfluidic devices to 3D porous media is unclear. Do the flow behaviors seen in 2D arise in 3D media as well? Emerging microfluidic techniques enable us to now answer this question—for example, using novel 3D fabrication methods¹⁹⁷ or using refractive index-matching of model 3D media.^{188,218–220}

Mixing and solute transport. The velocity fluctuations that characterize unstable flow of polymer solutions can also enhance mixing and solute dispersion on mesoscopic scales.^{22,160,221–225} This enhanced mixing could improve EOR and groundwater remediation efforts by improving the transport of key additives like surfactants, colloids, and oxidants. However, systematic tests of this behavior are lacking.

Enhanced mixing can be leveraged in other industrial processes as well. Mixing in microfluidic channels is typically diffusion-limited because of the low Reynolds numbers, but elastic flow instabilities have been shown to dramatically improve the speed of mixing.^{226,227} Similarly, this enhanced mixing can be leveraged for improved heat transfer in other industrial processes that require low Reynolds numbers.²²⁸

Other applications. Most studies focus on polymer solution flows in the context of oil

recovery and groundwater remediation. However, the work described in this review article may also be relevant to other applications that seek to use polymer solutions in porous media: filtration,²²⁹ fabrication of new materials, thin film processing,²³⁰ extrusion of polymers during 3D-printing,^{231,232} and novel forms of chromatography.²³³ Extending previous results to these new settings will be a useful direction for future research.

While we have focused on flows with $Re \ll 1$, many of these applications may involve $Re \geq 1$. How do the results obtained thus far extend to this new flow regime? Previous experiments shed some light on this question. Studies of flow through 1D arrays of posts shows that unstable upstream eddies form, similar to the low- Re case, when $Re \sim 20$.^{49,176,177} However, other experiments suggest that inertia suppresses temporal fluctuations of these eddies, and promotes symmetry in their structure; more generally, inertia appears to suppress the onset of elastic instabilities,^{48,164,166} in part due to scission of polymers.²³⁴

8 Acknowledgements

It is a pleasure to acknowledge P. D. Olmsted, R. K. Prud'homme, and H. A. Stone for stimulating discussions. Acknowledgment is made to the Donors of the American Chemical Society Petroleum Research Fund for partial support of this research. This material is also based upon work supported by the National Science Foundation Graduate Research Fellowship Program (to C.A.B.) under Grant No. DGE-1656466. Any opinions, findings, and conclusions or recommendations expressed in this material are those of the authors and do not necessarily reflect the views of the National Science Foundation. C.A.B. was supported in part by the Mary and Randall Hack Graduate Award of the Princeton Environmental Institute. A.S. was supported in part by the Lidow Thesis Fund at Princeton University and the Dede T. Bartlett P03 Fund for Student Research through the Andlinger Center for Energy and the Environment.



Christopher Browne is a Ph.D. candidate and NSF Graduate Research Fellow in Chemical and Biological Engineering at Princeton University. His research investigates how the unstable flow of polymer solutions develops in complex three-dimensional porous media. He earned his B.S. in Chemical Engineering from Purdue University.



Audrey Shih is a senior undergraduate at Princeton University pursuing a Bachelor's degree in Chemical and Biological Engineering and a certificate in Materials Science and Engineering. Her current research focuses on the influence of porous media geometry on polymer flow by using microfluidics to examine the link between chain conformations and macroscopic flow structure.



Sujit Datta is an Assistant Professor of Chemical and Biological Engineering at Princeton University. His lab's research focuses on the behavior of soft and active materials in complex settings, motivated by challenges like developing cleaner oil/gas recovery, more effective water remediation, and targeted drug delivery. Prof. Datta is the recipient of the LeRoy Apker Award from the American Physical Society, the Andreas Acrivos Award in Fluid Dynamics from the American Physical Society, the ACS Petroleum Research Fund New Investigator Award, the Alfred Rheinsein Faculty Award, and multiple Princeton Engineering Commendations for Outstanding Teaching.

References

- ¹ Kenneth S Sorbie. *Polymer-improved oil recovery*. Springer Science & Business Media, 2013.
- ² DS Roote. Technology status report: in situ flushing. *Ground Water Remediation Technology Analysis Center (available at <http://www.gwrtac.org>)*, 1998.
- ³ Qiang Liu, Mingzhe Dong, Shanzhou Ma, and Yun Tu. Surfactant enhanced alkaline flooding for western canadian heavy oil recovery. *Colloids and Surfaces A: Physicochemical and Engineering Aspects*, 293(1-3):63–71, 2007.
- ⁴ Nurudeen Yekeen, Ahmad Kamal Idris, Muhammad A Manan, Ali Mohamed Samin, Abdul Rahim Risal, and Tan Xin Kun. Bulk and bubble-scale experimental studies of influence of nanoparticles on foam stability. *Chinese Journal of Chemical Engineering*, 25(3):347–357, 2017.
- ⁵ Abhijit Samanta, Achinta Bera, Keka Ojha, and Ajay Mandal. Comparative studies on enhanced oil recovery by alkali–surfactant and polymer flooding. *Journal of Petroleum Exploration and Production Technology*, 2(2):67–74, 2012.
- ⁶ Afeez O Gbadamosi, Radzuan Junin, Muhammad A Manan, Nurudeen Yekeen, and Agi Augustine. Hybrid suspension of polymer and nanoparticles for enhanced oil recovery. *Polymer Bulletin*, pages 1–38, 2019.
- ⁷ Patrizio Raffa, Antonius A Broekhuis, and Francesco Picchioni. Polymeric surfactants for enhanced oil recovery: A review. *Journal of Petroleum Science and Engineering*, 145:723–733, 2016.
- ⁸ David F James and DR McLaren. The laminar flow of dilute polymer solutions through porous media. *Journal of Fluid Mechanics*, 70(4):733–752, 1975.
- ⁹ Demin Wang, Gang Wang, Huifen Xia, et al. Large scale high visco-elastic fluid flooding in the field achieves high recoveries. In *SPE Enhanced Oil Recovery Conference*. Society of Petroleum Engineers, 2011.
- ¹⁰ BB Sandiford et al. Laboratory and field studies of water floods using polymer solutions to increase oil recoveries. *Journal of Petroleum Technology*, 16(08):917–922, 1964.
- ¹¹ Malcolm J Pitts, Tom A Campbell, Harry Surkalo, Kon Wyatt, et al. Polymer flood of the rapdan pool, saskatchewan, canada. *SPE Reservoir Engineering*, 10(03):183–186, 1995.
- ¹² Bing Wei, Laura Romero-Zerón, and Denis Rodrigue. Oil displacement mechanisms of viscoelastic polymers in enhanced oil recovery (eor): a review. *Journal of Petroleum Exploration and Production Technology*, 4(2):113–121, 2014.
- ¹³ ECM Vermolen, MJT Van Haasterecht, SK Masalmeh, et al. A systematic study of the polymer visco-elastic effect on residual oil saturation by core flooding. In *SPE EOR Conference at Oil and Gas West Asia*. Society of Petroleum Engineers, 2014.

- ¹⁴ Andrew Clarke, Andrew M Howe, Jonathan Mitchell, John Staniland, Laurence A Hawkes, et al. How viscoelastic-polymer flooding enhances displacement efficiency. *SPE Journal*, 21(03):675–687, 2016.
- ¹⁵ Y Du, L Guan, et al. Field-scale polymer flooding: lessons learnt and experiences gained during past 40 years. In *SPE International Petroleum Conference in Mexico*. Society of Petroleum Engineers, 2004.
- ¹⁶ Simon J Haward and Jeffrey A Odell. Viscosity enhancement in non-newtonian flow of dilute polymer solutions through crystallographic porous media. *Rheologica acta*, 42(6):516–526, 2003.
- ¹⁷ JA Odell and SJ Haward. Viscosity enhancement in non-newtonian flow of dilute aqueous polymer solutions through crystallographic and random porous media. *Rheologica acta*, 45(6):853–863, 2006.
- ¹⁸ A Zaitoun, N Kohler, et al. Two-phase flow through porous media: effect of an adsorbed polymer layer. In *SPE Annual Technical Conference and Exhibition*. Society of Petroleum Engineers, 1988.
- ¹⁹ A Zaitoun, H Bertin, D Lasseux, et al. Two-phase flow property modifications by polymer adsorption. In *SPE/DOE improved oil recovery symposium*. Society of Petroleum Engineers, 1998.
- ²⁰ Chun Huh, Gary Arnold Pope, et al. Residual oil saturation from polymer floods: laboratory measurements and theoretical interpretation. In *SPE Symposium on Improved Oil Recovery*. Society of Petroleum Engineers, 2008.
- ²¹ JRA Pearson. Instability in non-newtonian flow. *Annual Review of Fluid Mechanics*, 8(1):163–181, 1976.
- ²² RG Larson. Flow-induced mixing, demixing, and phase transitions in polymeric fluids. *Rheologica Acta*, 31(6):497–520, 1992.
- ²³ Alexander Groisman and Victor Steinberg. Elastic turbulence in a polymer solution flow. *Nature*, 405(6782):53, 2000.
- ²⁴ MG Tsiklauri. Conditions for the occurrence of elastic turbulence in polymer solution flows through porous media. *Journal of engineering physics and thermophysics*, 66(3):233–239, 1994.
- ²⁵ Jonathan Mitchell, Kyle Lyons, Andrew M Howe, and Andrew Clarke. Viscoelastic polymer flows and elastic turbulence in three-dimensional porous structures. *Soft Matter*, 12(2):460–468, 2016.
- ²⁶ Martin J Blunt. *Multiphase flow in permeable media: A pore-scale perspective*. Cambridge University Press, 2017.

- ²⁷ Joseph D Seymour and Paul T Callaghan. Generalized approach to nmr analysis of flow and dispersion in porous media. *AIChE Journal*, 43(8):2096–2111, 1997.
- ²⁸ Ming Li, Laura Romero-Zerón, Florin Marica, and Bruce J Balcom. Polymer flooding enhanced oil recovery evaluated with magnetic resonance imaging and relaxation time measurements. *Energy & Fuels*, 31(5):4904–4914, 2017.
- ²⁹ Jennifer R Brown, Jacob Trudnowski, Elmira Nybo, Katherine E Kent, Thomas Lund, and Amanda Parsons. Quantification of non-newtonian fluid dynamics of a wormlike micelle solution in porous media with magnetic resonance. *Chemical Engineering Science*, 173:145–152, 2017.
- ³⁰ MD Shattuck, RP Behringer, GA Johnson, and John G Georgiadis. Convection and flow in porous media. part 1. visualization by magnetic resonance imaging. *Journal of Fluid Mechanics*, 332:215–245, 1997.
- ³¹ YE Kutsovsky, LE Scriven, HT Davis, and BE Hammer. Nmr imaging of velocity profiles and velocity distributions in bead packs. *Physics of Fluids*, 8(4):863–871, 1996.
- ³² L Lebon, L Oger, J Leblond, JP Hulin, NS Martys, and LM Schwartz. Pulsed gradient nmr measurements and numerical simulation of flow velocity distribution in sphere packings. *Physics of Fluids*, 8(2):293–301, 1996.
- ³³ L Lebon, J Leblond, and JP Hulin. Experimental measurement of dispersion processes at short times using a pulsed field gradient nmr technique. *Physics of Fluids*, 9(3):481–490, 1997.
- ³⁴ AJ Sederman, ML Johns, AS Bramley, P Alexander, and LF Gladden. Magnetic resonance imaging of liquid flow and pore structure within packed beds. *Chemical Engineering Science*, 52(14):2239–2250, 1997.
- ³⁵ AJ Sederman and LF Gladden. Mri as a probe of the deposition of solid fines in a porous medium. *Magnetic resonance imaging*, 19(3-4):565–567, 2001.
- ³⁶ DV Boger. Viscoelastic flows through contractions. *Annual review of fluid mechanics*, 19(1):157–182, 1987.
- ³⁷ GG Lipscomb II, Morton M Denn, DU Hur, and David V Boger. The flow of fiber suspensions in complex geometries. *Journal of Non-Newtonian Fluid Mechanics*, 26(3):297–325, 1988.
- ³⁸ A Mongrue and M Cloitre. Extensional flow of semidilute suspensions of rod-like particles through an orifice. *Physics Of Fluids*, 7(11):2546–2552, 1995.
- ³⁹ A Mongrue and M Cloitre. Axisymmetric orifice flow for measuring the elongational viscosity of semi-rigid polymer solutions. *Journal of non-newtonian fluid mechanics*, 110(1):27–43, 2003.

- ⁴⁰ Huaijiang Zhu, Jianhui Luo, Oldoerp Klaus, and Yongzhong Fan. The impact of extensional viscosity on oil displacement efficiency in polymer flooding. *Colloids and Surfaces A: Physicochemical and Engineering Aspects*, 414:498–503, 2012.
- ⁴¹ Tolknay Urbissinova, Japan J Trivedi, Ergun Kuru, et al. Effect of elasticity during viscoelastic polymer flooding-a possible mechanism of increasing the sweep efficiency. In *SPE western regional meeting*. Society of Petroleum Engineers, 2010.
- ⁴² Zhen Zhang, Jiachun Li, and Jifu Zhou. Microscopic roles of “viscoelasticity” in hpm polymer flooding for eor. *Transport in porous media*, 86(1):199–214, 2011.
- ⁴³ Ann Muggeridge, Andrew Cockin, Kevin Webb, Harry Frampton, Ian Collins, Tim Moulds, and Peter Salino. Recovery rates, enhanced oil recovery and technological limits. *Philosophical Transactions of the Royal Society A: Mathematical, Physical and Engineering Sciences*, 372(2006):20120320, 2014.
- ⁴⁴ Alimohammad Anbari, Hung-Ta Chien, Sujit S Datta, Wen Deng, David A Weitz, and Jing Fan. Microfluidic model porous media: fabrication and applications. *Small*, 14(18):1703575, 2018.
- ⁴⁵ Margaret G O’Connell, Nancy B Lu, Christopher A Browne, and Sujit S Datta. Cooperative size sorting of deformable particles in porous media. *Soft matter*, 15(17):3620–3626, 2019.
- ⁴⁶ William Thielicke and Eize Stamhuis. Pivlab—towards user-friendly, affordable and accurate digital particle image velocimetry in matlab. *Journal of Open Research Software*, 2(1), 2014.
- ⁴⁷ Martin J Blunt, Branko Bijeljic, Hu Dong, Oussama Gharbi, Stefan Iglauer, Peyman Mostaghimi, Adriana Paluszny, and Christopher Pentland. Pore-scale imaging and modelling. *Advances in Water Resources*, 51:197–216, 2013.
- ⁴⁸ LE Rodd, JJ Cooper-White, DV Boger, and GH McKinley. Role of the elasticity number in the entry flow of dilute polymer solutions in micro-fabricated contraction geometries. *Journal of Non-Newtonian Fluid Mechanics*, 143(2-3):170–191, 2007.
- ⁴⁹ Stephen Kenney, Kade Poper, Ganesh Chapagain, and Gordon F Christopher. Large Deborah number flows around confined microfluidic cylinders. *Rheologica Acta*, 52(5):485–497, 2013.
- ⁵⁰ Durgesh Kawale, Gelmer Bouwman, Shaurya Sachdev, Pacelli LJ Zitha, Michiel T Kreutzer, William R Rossen, and Pouyan E Boukany. Polymer conformation during flow in porous media. *Soft matter*, 13(46):8745–8755, 2017.
- ⁵¹ Michael A Nilsson, Ruta Kulkarni, Lauren Gerberich, Ryan Hammond, Rohitashwa Singh, Elizabeth Baumhoff, and Jonathan P Rothstein. Effect of fluid rheology on enhanced oil recovery in a microfluidic sandstone device. *Journal of Non-Newtonian Fluid Mechanics*, 202:112–119, 2013.

- ⁵² Thomas J Ober, Simon J Haward, Christopher J Pipe, Johannes Soulages, and Gareth H McKinley. Microfluidic extensional rheometry using a hyperbolic contraction geometry. *Rheologica Acta*, 52(6):529–546, 2013.
- ⁵³ William Walter Graessley. *Polymeric liquids and networks: dynamics and rheology*. Garland Science, 2008.
- ⁵⁴ Matthew T Balhoff and Karsten E Thompson. A macroscopic model for shear-thinning flow in packed beds based on network modeling. *Chemical Engineering Science*, 61(2):698–719, 2006.
- ⁵⁵ Frédéric Zami-Pierre, R De Loubens, Michel Quintard, and Yohan Davit. Transition in the flow of power-law fluids through isotropic porous media. *Physical review letters*, 117(7):074502, 2016.
- ⁵⁶ Anaïs Machado, Hugues Bodiguel, Julien Beaumont, Gérald Clisson, and Annie Colin. Extra dissipation and flow uniformization due to elastic instabilities of shear-thinning polymer solutions in model porous media. *Biomicrofluidics*, 10(4):043507, 2016.
- ⁵⁷ GK Batchelor. The stress generated in a non-dilute suspension of elongated particles by pure straining motion. *Journal of Fluid Mechanics*, 46(4):813–829, 1971.
- ⁵⁸ Andrey V Dobrynin, Ralph H Colby, and Michael Rubinstein. Scaling theory of polyelectrolyte solutions. *Macromolecules*, 28(6):1859–1871, 1995.
- ⁵⁹ Emre Turkoz, Antonio Perazzo, Craig B Arnold, and Howard A Stone. Salt type and concentration affect the viscoelasticity of polyelectrolyte solutions. *Applied Physics Letters*, 112(20):203701, 2018.
- ⁶⁰ Durgesh Kawale, Esteban Marques, Pacelli LJ Zitha, Michiel T Kreutzer, William R Rossen, and Pouyan E Boukany. Elastic instabilities during the flow of hydrolyzed polyacrylamide solution in porous media: Effect of pore-shape and salt. *Soft matter*, 13(4):765–775, 2017.
- ⁶¹ Gerald G Fuller, Cheryl A Cathey, Brent Hubbard, and Beth E Zebrowski. Extensional viscosity measurements for low-viscosity fluids. *Journal of Rheology*, 31(3):235–249, 1987.
- ⁶² Cheryl A Cathey and Gerald G Fuller. Uniaxial and biaxial extensional viscosity measurements of dilute and semi-dilute solutions of rigid rod polymers. *Journal of non-newtonian fluid mechanics*, 30(2-3):303–316, 1988.
- ⁶³ Leidy Nallely Jimenez, Jelena Dinic, Nikhila Parsi, and Vivek Sharma. Extensional relaxation time, pinch-off dynamics, and printability of semidilute polyelectrolyte solutions. *Macromolecules*, 51(14):5191–5208, 2018.
- ⁶⁴ Anna V Walter, Leidy N Jimenez, Jelena Dinic, Vivek Sharma, and Kendra A Erk. Effect of salt valency and concentration on shear and extensional rheology of aqueous polyelectrolyte solutions for enhanced oil recovery. *Rheologica Acta*, 58(3-4):145–157, 2019.

- ⁶⁵ Francesco Del Giudice, Simon J Haward, and Amy Q Shen. Relaxation time of dilute polymer solutions: A microfluidic approach. *Journal of Rheology*, 61(2):327–337, 2017.
- ⁶⁶ SJ Haward. Microfluidic extensional rheometry using stagnation point flow. *Biomicrofluidics*, 10(4):043401, 2016.
- ⁶⁷ Gabriel Juarez and Paulo E Arratia. Extensional rheology of dna suspensions in microfluidic devices. *Soft Matter*, 7(19):9444–9452, 2011.
- ⁶⁸ François Ingremeau and Hamid Kellay. Stretching polymers in droplet-pinch-off experiments. *Physical Review X*, 3(4):041002, 2013.
- ⁶⁹ Shaurya Sachdev, Aswin Muralidharan, and Pouyan E Boukany. Molecular processes leading to “necking” in extensional flow of polymer solutions: Using microfluidics and single dna imaging. *Macromolecules*, 49(24):9578–9585, 2016.
- ⁷⁰ Seo Gyun Kim, Chang Min Ok, and Heon Sang Lee. Steady-state extensional viscosity of a linear polymer solution using a differential pressure extensional rheometer on a chip. *Journal of Rheology*, 62(5):1261–1270, 2018.
- ⁷¹ R Byron Bird, Robert C Armstrong, and Ole Hassager. *Dynamics of polymeric liquids. Volume 1: fluid mechanics*. A Wiley-Interscience Publication, John Wiley & Sons, 1987.
- ⁷² A Peterlin. Streaming birefringence of soft linear macromolecules with finite chain length. *Polymer*, 2:257–264, 1961.
- ⁷³ K Weissenberg. A continuum theory of rheological phenomena, 1947.
- ⁷⁴ Andrew M Howe, Andrew Clarke, and Daniel Giernalczyk. Flow of concentrated viscoelastic polymer solutions in porous media: effect of mw and concentration on elastic turbulence onset in various geometries. *Soft Matter*, 11(32):6419–6431, 2015.
- ⁷⁵ Christopher W Macosko and Ronald G Larson. *Rheology: principles, measurements, and applications*. Vch New York, 1994.
- ⁷⁶ JM Dealy. Weissenberg and Deborah numbers—their definition and use. *Rheol. Bull*, 79(2):14–18, 2010.
- ⁷⁷ RJ Poole. The Deborah and Weissenberg numbers. *British Soc. Rheol. Rheol. Bull*, 53:32–39, 2012.
- ⁷⁸ Kyu Hyun, Manfred Wilhelm, Christopher O Klein, Kwang Soo Cho, Jung Gun Nam, Kyung Hyun Ahn, Seung Jong Lee, Randy H Ewoldt, and Gareth H McKinley. A review of nonlinear oscillatory shear tests: Analysis and application of large amplitude oscillatory shear (laos). *Progress in Polymer Science*, 36(12):1697–1753, 2011.
- ⁷⁹ Simon Rogers. Large amplitude oscillatory shear: simple to describe, hard to interpret. *Physics Today*, 71(7):34–40, 2018.

- ⁸⁰ L-S Cheng and R-Y Cao. Constitutive model of viscous-elastic polymer solution in porous media. *Petroleum Science and Technology*, 28(11):1170–1177, 2010.
- ⁸¹ David A Hoagland and RK Prud’Homme. Hydrodynamic chromatography as a probe of polymer dynamics during flow through porous media. *Macromolecules*, 22(2):775–781, 1989.
- ⁸² PG De Gennes. Scaling theory of polymer adsorption. *Journal de physique*, 37(12):1445–1452, 1976.
- ⁸³ Pacelli LJ Zitha, Guy Chauveteau, and Liliane Léger. Unsteady-state flow of flexible polymers in porous media. *Journal of colloid and interface science*, 234(2):269–283, 2001.
- ⁸⁴ Hazen P Babcock, Rodrigo E Teixeira, Joe S Hur, Eric SG Shaqfeh, and Steven Chu. Visualization of molecular fluctuations near the critical point of the coil- stretch transition in polymer elongation. *Macromolecules*, 36(12):4544–4548, 2003.
- ⁸⁵ Charles M Schroeder, Hazen P Babcock, Eric SG Shaqfeh, and Steven Chu. Observation of polymer conformation hysteresis in extensional flow. *Science*, 301(5639):1515–1519, 2003.
- ⁸⁶ Timothy M Obey and PC Griffiths. Polymer adsorption: Fundamentals. *COSMETIC SCIENCE AND TECHNOLOGY SERIES*, pages 51–72, 1999.
- ⁸⁷ M Rubenstein and RH Colby. *Polymer physics: Oxford university press*. Oxford, UK, 2003.
- ⁸⁸ P Zitha, G Chauveteau, A Zaitoun, et al. Permeability~ dependent propagation of polyacrylamides under near-wellbore flow conditions. In *SPE International Symposium on Oilfield Chemistry*. Society of Petroleum Engineers, 1995.
- ⁸⁹ Mohamed IM Darwish, John E McCray, Peter K Currie, and Pacelli LJ Zitha. Polymer-enhanced dnapl flushing from low-permeability media: An experimental study. *Ground-water Monitoring & Remediation*, 23(2):92–101, 2003.
- ⁹⁰ CA Grattoni, PF Luckham, XD Jing, L Norman, and Robert W Zimmerman. Polymers as relative permeability modifiers: adsorption and the dynamic formation of thick polyacrylamide layers. *Journal of petroleum science and engineering*, 45(3-4):233–245, 2004.
- ⁹¹ G Chauveteau and M Moan. The onset of dilatant behaviour in non-inertial flow of dilute polymer solutions through channels with varying cross-sections. *Journal de Physique Lettres*, 42(10):201–204, 1981.
- ⁹² G Chauveteau, M Moan, and A Magueur. Thickening behaviour of dilute polymer solutions in non-inertial elongational flows. *Journal of non-newtonian fluid mechanics*, 16(3):315–327, 1984.

- ⁹³ R Prabhakar, Papanasamoorthy Sunthar, and J Ravi Prakash. Exploring the universal dynamics of dilute polymer solutions in extensional flows. *Physica A: Statistical Mechanics and its Applications*, 339(1-2):34–39, 2004.
- ⁹⁴ Rahul K Gupta, DA Nguyen, and T Sridhar. Extensional viscosity of dilute polystyrene solutions: Effect of concentration and molecular weight. *Physics of Fluids*, 12(6):1296–1318, 2000.
- ⁹⁵ Douglas E Smith and Steven Chu. Response of flexible polymers to a sudden elongational flow. *Science*, 281(5381):1335–1340, 1998.
- ⁹⁶ Stergios Pilitsis and Antony N Beris. Calculations of steady-state viscoelastic flow in an undulating tube. *Journal of Non-Newtonian Fluid Mechanics*, 31(3):231–287, 1989.
- ⁹⁷ Stergios Pilitsis and Antony N Beris. Viscoelastic flow in an undulating tube. part ii. effects of high elasticity, large amplitude of undulation and inertia. *Journal of non-newtonian fluid mechanics*, 39(3):375–405, 1991.
- ⁹⁸ Kapil K Talwar and Bamin Khomami. Flow of viscoelastic fluids past periodic square arrays of cylinders: inertial and shear thinning viscosity and elasticity effects. *Journal of Non-Newtonian Fluid Mechanics*, 57(2-3):177–202, 1995.
- ⁹⁹ Hays S Rye, Jonathan M Dabora, Mark A Quesada, Richard A Mathies, and Alexander N Glazer. Fluorometric assay using dimeric dyes for double-and single-stranded dna and rna with picogram sensitivity. *Analytical biochemistry*, 208(1):144–150, 1993.
- ¹⁰⁰ Nerayo P Teclemariam, Victor A Beck, Eric SG Shaqfeh, and Susan J Muller. Dynamics of dna polymers in post arrays: Comparison of single molecule experiments and simulations. *Macromolecules*, 40(10):3848–3859, 2007.
- ¹⁰¹ Orin L Hemminger, Pouyan E Boukany, Shi-Qing Wang, and LJ Lee. Flow pattern and molecular visualization of dna solutions through a 4: 1 planar micro-contraction. *Journal of Non-Newtonian Fluid Mechanics*, 165(23-24):1613–1624, 2010.
- ¹⁰² Thomas T Perkins, Douglas E Smith, and Steven Chu. Single polymer dynamics in an elongational flow. *Science*, 276(5321):2016–2021, 1997.
- ¹⁰³ Lea Rems, Durgesh Kawale, L James Lee, and Pouyan E Boukany. Flow of dna in micro/nanofluidics: From fundamentals to applications. *Biomicrofluidics*, 10(4):043403, 2016.
- ¹⁰⁴ Charles M Schroeder. Single polymer dynamics for molecular rheology. *Journal of Rheology*, 62(1):371–403, 2018.
- ¹⁰⁵ Nicolas François, David Lasne, Yacine Amarouchene, Brahim Lounis, and Hamid Kellay. Drag enhancement with polymers. *Physical review letters*, 100(1):018302, 2008.
- ¹⁰⁶ Nicolas François, Yacine Amarouchene, Brahim Lounis, and Hamid Kellay. Polymer conformations and hysteretic stresses in nonstationary flows of polymer solutions. *EPL (Europhysics Letters)*, 86(3):34002, 2009.

- ¹⁰⁷ PG De Gennes. Coil-stretch transition of dilute flexible polymers under ultrahigh velocity gradients. *The Journal of Chemical Physics*, 60(12):5030–5042, 1974.
- ¹⁰⁸ GG Fuller and LG Leal. Flow birefringence of dilute polymer solutions in two-dimensional flows. *Rheologica Acta*, 19(5):580–600, 1980.
- ¹⁰⁹ D Hunkeler, TQ Nguyen, and HH Kausch. Polymer solutions under elongational flow: 1. birefringence characterization of transient and stagnation point elongational flows. *Polymer*, 37(19):4257–4269, 1996.
- ¹¹⁰ Malika J Menasveta and David A Hoagland. Light scattering from dilute poly (styrene) solutions in uniaxial elongational flow. *Macromolecules*, 24(11):3427–3433, 1991.
- ¹¹¹ R Blake Goff, Steven F Karel, and Robert K Prud’homme. Electric birefringence of flexible polymers in high fields: Brownian dynamics simulation. *The Journal of chemical physics*, 100(3):2289–2297, 1994.
- ¹¹² S Gerashchenko, C Chevallard, and V Steinberg. Single-polymer dynamics: Coil-stretch transition in a random flow. *EPL (Europhysics Letters)*, 71(2):221, 2005.
- ¹¹³ RI Tanner. Stresses in dilute solutions of bead-nonlinear-spring macromolecules. iii. friction coefficient varying with dumbbell extension. *Transactions of the Society of Rheology*, 19(4):557–582, 1975.
- ¹¹⁴ JJ Magda, RG Larson, and ME Mackay. Deformation-dependent hydrodynamic interaction in flows of dilute polymer solutions. *The Journal of chemical physics*, 89(4):2504–2513, 1988.
- ¹¹⁵ JM Rallison and EJ Hinch. Do we understand the physics in the constitutive equation? *Journal of Non-Newtonian Fluid Mechanics*, 29:37–55, 1988.
- ¹¹⁶ Yonggang Liu, Yonggun Jun, and Victor Steinberg. Longest relaxation times of double-stranded and single-stranded dna. *Macromolecules*, 40(6):2172–2176, 2007.
- ¹¹⁷ Kai-Wen Hsiao, Chandi Sasmal, J Ravi Prakash, and Charles M Schroeder. Direct observation of dna dynamics in semidilute solutions in extensional flow. *Journal of Rheology*, 61(1):151–167, 2017.
- ¹¹⁸ Joe S Hur, Eric SG Shaqfeh, Hazen P Babcock, Douglas E Smith, and Steven Chu. Dynamics of dilute and semidilute dna solutions in the start-up of shear flow. *Journal of Rheology*, 45(2):421–450, 2001.
- ¹¹⁹ Teh Chung Ho and Morton M Denn. Stability of plane poiseuille flow of a highly elastic liquid. *Journal of Non-Newtonian Fluid Mechanics*, 3(2):179–195, 1977.
- ¹²⁰ Jeffrey A Byars, Alparslan Öztekin, Robert A Brown, and Gareth H Mckinley. Spiral instabilities in the flow of highly elastic fluids between rotating parallel disks. *Journal of Fluid Mechanics*, 271:173–218, 1994.

- ¹²¹ Laura Casanellas, Manuel A Alves, Robert J Poole, Sandra Lerouge, and Anke Lindner. The stabilizing effect of shear thinning on the onset of purely elastic instabilities in serpentine microflows. *Soft matter*, 12(29):6167–6175, 2016.
- ¹²² Jyoti Chakraborty, Nishith Verma, and RP Chhabra. Wall effects in flow past a circular cylinder in a plane channel: a numerical study. *Chemical Engineering and Processing: Process Intensification*, 43(12):1529–1537, 2004.
- ¹²³ Francisco J Galindo-Rosales, Laura Campo-Deaño, FT Pinho, E Van Bokhorst, PJ Hamersma, Mónica SN Oliveira, and MA Alves. Microfluidic systems for the analysis of viscoelastic fluid flow phenomena in porous media. *Microfluidics and nanofluidics*, 12(1-4):485–498, 2012.
- ¹²⁴ Francisco J Galindo-Rosales, Laura Campo-Deaño, Patrícia C Sousa, Vera M Ribeiro, Mónica SN Oliveira, Manuel A Alves, and Fernando T Pinho. Viscoelastic instabilities in micro-scale flows. *Experimental Thermal and Fluid Science*, 59:128–139, 2014.
- ¹²⁵ Simon J Haward, Gareth H McKinley, and Amy Q Shen. Elastic instabilities in planar elongational flow of monodisperse polymer solutions. *Scientific reports*, 6:33029, 2016.
- ¹²⁶ Martien A Hulsen, Raanan Fattal, and Raz Kupferman. Flow of viscoelastic fluids past a cylinder at high weissenberg number: stabilized simulations using matrix logarithms. *Journal of Non-Newtonian Fluid Mechanics*, 127(1):27–39, 2005.
- ¹²⁷ Ronald G Larson. Instabilities in viscoelastic flows. *Rheologica Acta*, 31(3):213–263, 1992.
- ¹²⁸ Susan J Muller, Ronald G Larson, and Eric SG Shaqfeh. A purely elastic transition in taylor-couette flow. *Rheologica Acta*, 28(6):499–503, 1989.
- ¹²⁹ Ronald G Larson, Eric SG Shaqfeh, and Susan J Muller. A purely elastic instability in taylor-couette flow. *Journal of Fluid Mechanics*, 218:573–600, 1990.
- ¹³⁰ T Lee and R Budwig. A study of the effect of aspect ratio on vortex shedding behind circular cylinders. *Physics of Fluids A: Fluid Dynamics*, 3(2):309–315, 1991.
- ¹³¹ Xiao-Bin Li, Feng-Chen Li, Wei-Hua Cai, Hong-Na Zhang, and Juan-Cheng Yang. Very-low-re chaotic motions of viscoelastic fluid and its unique applications in microfluidic devices: a review. *Experimental thermal and fluid science*, 39:1–16, 2012.
- ¹³² JJ Magda and RG Larson. A transition occurring in ideal elastic liquids during shear flow. *Journal of non-newtonian fluid mechanics*, 30(1):1–19, 1988.
- ¹³³ Gareth H McKinley, Robert C Armstrong, and Robert Brown. The wake instability in viscoelastic flow past confined circular cylinders. *Philosophical Transactions of the Royal Society of London. Series A: Physical and Engineering Sciences*, 344(1671):265–304, 1993.
- ¹³⁴ Gareth H McKinley, Jeffrey A Byars, Robert A Brown, and Robert C Armstrong. Observations on the elastic instability in cone-and-plate and parallel-plate flows of a polyisobutylene boger fluid. *Journal of Non-Newtonian Fluid Mechanics*, 40(2):201–229, 1991.

- ¹³⁵ Gareth H Mckinley, Alparslan Öztekin, Jeffrey A Byars, and Robert A Brown. Self-similar spiral instabilities in elastic flows between a cone and a plate. *Journal of Fluid Mechanics*, 285:123–164, 1995.
- ¹³⁶ Paulo J Oliveira and Amílcar IP Miranda. A numerical study of steady and unsteady viscoelastic flow past bounded cylinders. *Journal of non-newtonian fluid mechanics*, 127(1):51–66, 2005.
- ¹³⁷ MSN Oliveira, FT Pinho, RJ Poole, PJ Oliveira, and MA Alves. Purely elastic flow asymmetries in flow-focusing devices. *Journal of Non-Newtonian Fluid Mechanics*, 160(1):31–39, 2009.
- ¹³⁸ RJ Poole, MA Alves, and Paulo J Oliveira. Purely elastic flow asymmetries. *Physical review letters*, 99(16):164503, 2007.
- ¹³⁹ Jai A Pathak, David Ross, and Kalman B Migler. Elastic flow instability, curved streamlines, and mixing in microfluidic flows. *Physics of fluids*, 16(11):4028–4034, 2004.
- ¹⁴⁰ VM Ribeiro, PM Coelho, FT Pinho, and MA Alves. Viscoelastic fluid flow past a confined cylinder: Three-dimensional effects and stability. *Chemical engineering science*, 111:364–380, 2014.
- ¹⁴¹ Subhankar Sen, Sanjay Mittal, and Gautam Biswas. Steady separated flow past a circular cylinder at low reynolds numbers. *Journal of Fluid Mechanics*, 620:89–119, 2009.
- ¹⁴² Eric SG Shaqfeh. Purely elastic instabilities in viscometric flows. *Annual Review of Fluid Mechanics*, 28(1):129–185, 1996.
- ¹⁴³ Charles HK Williamson. Vortex dynamics in the cylinder wake. *Annual review of fluid mechanics*, 28(1):477–539, 1996.
- ¹⁴⁴ Helen J Wilson, Michael Renardy, and Yuriko Renardy. Structure of the spectrum in zero reynolds number shear flow of the ucm and oldroyd-b liquids. *Journal of non-newtonian fluid mechanics*, 80(2-3):251–268, 1999.
- ¹⁴⁵ MD Chilcott and JM Rallison. Creeping flow of dilute polymer solutions past cylinders and spheres. *Journal of non-newtonian fluid mechanics*, 29:381–432, 1988.
- ¹⁴⁶ Simon J Haward, Naoyuki Kitajima, Kazumi Toda-Peters, Tsutomu Takahashi, and Amy Q Shen. Flow of wormlike micellar solutions around microfluidic cylinders with high aspect ratio and low blockage ratio. *Soft Matter*, 15:1927–1941, 2019.
- ¹⁴⁷ Boyang Qin and Paulo E Arratia. Characterizing elastic turbulence in channel flows at low reynolds number. *Physical Review Fluids*, 2(8):083302, 2017.
- ¹⁴⁸ S Berti, A Bistagnino, Guido Boffetta, A Celani, and S Musacchio. Two-dimensional elastic turbulence. *Physical Review E*, 77(5):055306, 2008.

- ¹⁴⁹ Muzio Grilli, Adolfo Vázquez-Quesada, and Marco Ellero. Transition to turbulence and mixing in a viscoelastic fluid flowing inside a channel with a periodic array of cylindrical obstacles. *Physical review letters*, 110(17):174501, 2013.
- ¹⁵⁰ Frédéric Zami-Pierre, R de Loubens, Michel Quintard, and Yohan Davit. Polymer flow through porous media: numerical prediction of the contribution of slip to the apparent viscosity. *Transport in Porous Media*, 119(3):521–538, 2017.
- ¹⁵¹ Guido Boffetta, Antonio Celani, and Stefano Musacchio. Two-dimensional turbulence of dilute polymer solutions. *Physical review letters*, 91(3):034501, 2003.
- ¹⁵² Yonggang Liu and Victor Steinberg. Single polymer dynamics in a random flow. In *Macromolecular Symposia*, volume 337, pages 34–43. Wiley Online Library, 2014.
- ¹⁵³ SJ Haward and GH McKinley. Instabilities in stagnation point flows of polymer solutions. *Physics of Fluids*, 25(8):083104, 2013.
- ¹⁵⁴ PC Sousa, FT Pinho, MSN Oliveira, and MA Alves. Purely elastic flow instabilities in microscale cross-slot devices. *Soft matter*, 11(45):8856–8862, 2015.
- ¹⁵⁵ Alfredo Lanzaro, Daniel Corbett, and Xue-Feng Yuan. Non-linear dynamics of semi-dilute paam solutions in a microfluidic 3d cross-slot flow geometry. *Journal of Non-Newtonian Fluid Mechanics*, 242:57–65, 2017.
- ¹⁵⁶ Mihailo R Jovanović and Satish Kumar. Nonmodal amplification of stochastic disturbances in strongly elastic channel flows. *Journal of Non-Newtonian Fluid Mechanics*, 166(14-15):755–778, 2011.
- ¹⁵⁷ Paulo E Arratia, CC Thomas, J Diorio, and Jerry P Gollub. Elastic instabilities of polymer solutions in cross-channel flow. *Physical review letters*, 96(14):144502, 2006.
- ¹⁵⁸ L Pan, A Morozov, C Wagner, and PE Arratia. Nonlinear elastic instability in channel flows at low reynolds numbers. *Physical review letters*, 110(17):174502, 2013.
- ¹⁵⁹ Peyman Pakdel and Gareth H McKinley. Elastic instability and curved streamlines. *Physical Review Letters*, 77(12):2459, 1996.
- ¹⁶⁰ Boyang Qin, Paul F Salipante, Steven D Hudson, and Paulo E Arratia. Flow resistance and structures in viscoelastic channel flows at low re. *arXiv preprint arXiv:1807.00927*, 2018.
- ¹⁶¹ Gareth H McKinley, Peyman Pakdel, and Alparslan Öztekin. Rheological and geometric scaling of purely elastic flow instabilities. *Journal of Non-Newtonian Fluid Mechanics*, 67:19–47, 1996.
- ¹⁶² J Zilz, RJ Poole, MA Alves, D Bartolo, B Levaché, and A Lindner. Geometric scaling of a purely elastic flow instability in serpentine channels. *Journal of Fluid Mechanics*, 712:203–218, 2012.

- ¹⁶³ Alfredo Lanzaro and Xue-Feng Yuan. Effects of contraction ratio on non-linear dynamics of semi-dilute, highly polydisperse paam solutions in microfluidics. *Journal of Non-Newtonian Fluid Mechanics*, 166(17-18):1064–1075, 2011.
- ¹⁶⁴ Lucy E Rodd, Timothy P Scott, David V Boger, Justin J Cooper-White, and Gareth H McKinley. The inertio-elastic planar entry flow of low-viscosity elastic fluids in micro-fabricated geometries. *Journal of Non-Newtonian Fluid Mechanics*, 129(1):1–22, 2005.
- ¹⁶⁵ KW Koelling and Robert Krafft Prud’homme. Instabilities in multi-hole converging flow of viscoelastic fluids. *Rheologica acta*, 30(6):511–522, 1991.
- ¹⁶⁶ Alfredo Lanzaro. *Microscopic flows of aqueous polyacrylamide solutions: a quantitative study*. PhD thesis, The University of Manchester (United Kingdom), 2011.
- ¹⁶⁷ Alfredo Lanzaro and Xue-Feng Yuan. A quantitative analysis of spatial extensional rate distribution in nonlinear viscoelastic flows. *Journal of Non-Newtonian Fluid Mechanics*, 207:32–41, 2014.
- ¹⁶⁸ Alfredo Lanzaro, Zhuo Li, and Xue-Feng Yuan. Quantitative characterization of high molecular weight polymer solutions in microfluidic hyperbolic contraction flow. *Microfluidics and Nanofluidics*, 18(5-6):819–828, 2015.
- ¹⁶⁹ Shelly Gulati, Susan J Muller, and Dorian Liepmann. Flow of dna solutions in a microfluidic gradual contraction. *Biomicrofluidics*, 9(5):054102, 2015.
- ¹⁷⁰ Peter Szabo, JM Rallison, and EJ Hinch. Start-up of flow of a fene-fluid through a 4: 1: 4 constriction in a tube. *Journal of non-newtonian fluid mechanics*, 72(1):73–86, 1997.
- ¹⁷¹ Boyang Qin, Paul F Salipante, Steven D Hudson, and Paulo E Arratia. Upstream vortex and elastic wave in the viscoelastic flow around a confined cylinder. *Journal of Fluid Mechanics*, 864, 2019.
- ¹⁷² Atul Varshney and Victor Steinberg. Elastic wake instabilities in a creeping flow between two obstacles. *Physical Review Fluids*, 2(5):051301, 2017.
- ¹⁷³ Simon J Haward, Kazumi Toda-Peters, and Amy Q Shen. Steady viscoelastic flow around high-aspect-ratio, low-blockage-ratio microfluidic cylinders. *Journal of Non-Newtonian Fluid Mechanics*, 254:23–35, 2018.
- ¹⁷⁴ Barnin Khomami and Luis D Moreno. Stability of viscoelastic flow around periodic arrays of cylinders. *Rheologica acta*, 36(4):367–383, 1997.
- ¹⁷⁵ K Arora, R Sureshkumar, and B Khomami. Experimental investigation of purely elastic instabilities in periodic flows. *Journal of non-newtonian fluid mechanics*, 108(1-3):209–226, 2002.
- ¹⁷⁶ Xueda Shi, Stephen Kenney, Ganesh Chapagain, and Gordon F Christopher. Mechanisms of onset for moderate mach number instabilities of viscoelastic flows around confined cylinders. *Rheologica Acta*, 54(9-10):805–815, 2015.

- ¹⁷⁷ Xueda Shi and Gordon F Christopher. Growth of viscoelastic instabilities around linear cylinder arrays. *Physics of Fluids*, 28(12):124102, 2016.
- ¹⁷⁸ Durgesh Kawale, Jishnu Jayaraman, and Pouyan E Boukany. Microfluidic rectifier for polymer solutions flowing through porous media. *Biomicrofluidics*, 13(1):014111, 2019.
- ¹⁷⁹ S De, J van der Schaaf, NG Deen, JAM Kuipers, EAJF Peters, and JT Padding. Lane change in flows through pillared microchannels. *Physics of Fluids*, 29:113102 1–8, 2017.
- ¹⁸⁰ S De, P Krishnan, J van der Schaaf, JAM Kuipers, EAJF Peters, and JT Padding. Viscoelastic effects on residual oil distribution in flows through pillared microchannels. *Journal of colloid and interface science*, 510:262–271, 2018.
- ¹⁸¹ B Sadanandan and Radhakrishna Sureshkumar. Global linear stability analysis of viscoelastic flow through a periodic channel. *Journal of non-newtonian fluid mechanics*, 122(1-3):55–67, 2004.
- ¹⁸² S De, S Das, JAM Kuipers, EAJF Peters, and JT Padding. A coupled finite volume immersed boundary method for simulating 3d viscoelastic flows in complex geometries. *Journal of Non-Newtonian Fluid Mechanics*, 232:67–76, 2016.
- ¹⁸³ S De, JAM Kuipers, EAJF Peters, and JT Padding. Viscoelastic flow simulations in model porous media. *Physical Review Fluids*, 2(5):053303, 2017.
- ¹⁸⁴ A Vázquez-Quesada and M Ellero. Sph simulations of a viscoelastic flow around a periodic array of cylinders confined in a channel. *Journal of Non-Newtonian Fluid Mechanics*, 167:1–8, 2012.
- ¹⁸⁵ S De, JAM Kuipers, EAJF Peters, and JT Padding. Viscoelastic flow simulations in random porous media. *Journal of Non-Newtonian Fluid Mechanics*, 248:50–61, 2017.
- ¹⁸⁶ Shauvik De, Johannes AM Kuipers, Elias AJF Peters, and Johan T Padding. Viscoelastic flow past mono-and bidisperse random arrays of cylinders: flow resistance, topology and normal stress distribution. *Soft matter*, 13(48):9138–9146, 2017.
- ¹⁸⁷ Derek M Walkama, Nicolas Waisbord, and Jeffrey S Guasto. Disorder suppresses chaos in viscoelastic flows. *arXiv preprint arXiv:1906.11868*, 2019.
- ¹⁸⁸ Sujit S Datta, TS Ramakrishnan, and David A Weitz. Mobilization of a trapped non-wetting fluid from a three-dimensional porous medium. *Physics of Fluids*, 26(2):022002, 2014.
- ¹⁸⁹ NR Morrow, I Chatzis, JJ Taber, et al. Entrapment and mobilization of residual oil in bead packs. *SPE Reservoir Engineering*, 3(03):927–934, 1988.
- ¹⁹⁰ P Amili and YC Yortsos. Darcian dynamics: a new approach to the mobilization of a trapped phase in porous media. *Transport in porous media*, 64(1):25–49, 2006.

- ¹⁹¹ Demin Wang, Huifen Xia, Shuren Yang, Gang Wang, et al. The influence of visco-elasticity on micro forces and displacement efficiency in pores, cores and in the field. In *SPE EOR Conference at Oil & Gas West Asia*. Society of Petroleum Engineers, 2010.
- ¹⁹² Steven W Giese and Susan E Powers. Using polymer solutions to enhance recovery of mobile coal tar and creosote dnaps. *Journal of contaminant hydrology*, 58(1-2):147–167, 2002.
- ¹⁹³ Megan M Smith, Jeff AK Silva, Junko Munakata-Marr, and John E McCray. Compatibility of polymers and chemical oxidants for enhanced groundwater remediation. *Environmental science & technology*, 42(24):9296–9301, 2008.
- ¹⁹⁴ FRBU Durst, R Haas, and BU Kaczmar. Flows of dilute hydrolyzed polyacrylamide solutions in porous media under various solvent conditions. *Journal of Applied Polymer Science*, 26(9):3125–3149, 1981.
- ¹⁹⁵ FN Schneider, WW Owens, et al. Steady-state measurements of relative permeability for polymer/oil systems. *Society of Petroleum Engineers Journal*, 22(01):79–86, 1982.
- ¹⁹⁶ K Sandengen, MT Tweheyo, CM Crescente, A Mouret, I Henaut, and D Rousseau. Qualifying an “emulsion” polymer for field use-lab-scale assessments on adsorption and injectivity. In *IOR 2017-19th European Symposium on Improved Oil Recovery*, 2017.
- ¹⁹⁷ Ke Xu, Tianbo Liang, Peixi Zhu, Pengpeng Qi, Jun Lu, Chun Huh, and Matthew Balhoff. A 2.5-d glass micromodel for investigation of multi-phase flow in porous media. *Lab on a Chip*, 17(4):640–646, 2017.
- ¹⁹⁸ Mike Lacey, Cathy Hollis, Mart Oostrom, and Nima Shokri. Effects of pore and grain size on water and polymer flooding in micromodels. *Energy & Fuels*, 31(9):9026–9034, 2017.
- ¹⁹⁹ J Avendano, Nicolas Pannacci, Benjamin Herzhaft, Patrick Gateau, and P Coussot. Enhanced displacement of a liquid pushed by a viscoelastic fluid. *Journal of colloid and interface science*, 410:172–180, 2013.
- ²⁰⁰ JG Roof et al. Snap-off of oil droplets in water-wet pores. *Society of Petroleum Engineers Journal*, 10(01):85–90, 1970.
- ²⁰¹ Ladislav Derzsi, Marta Kasprzyk, Jan Philip Plog, and Piotr Garstecki. Flow focusing with viscoelastic liquids. *Physics of Fluids*, 25(9):092001, 2013.
- ²⁰² Anupam Gupta and Mauro Sbragaglia. Effects of viscoelasticity on droplet dynamics and break-up in microfluidic t-junctions: a lattice boltzmann study. *The European Physical Journal E*, 39(1):6, 2016.
- ²⁰³ Mohammad Nooranidoost, Daulet Izbassarov, and Metin Muradoglu. Droplet formation in a flow focusing configuration: Effects of viscoelasticity. *Physics of Fluids*, 28(12):123102, 2016.

- ²⁰⁴ Mehdi Nekouei and Siva A Vanapalli. Volume-of-fluid simulations in microfluidic t-junction devices: Influence of viscosity ratio on droplet size. *Physics of Fluids*, 29(3):032007, 2017.
- ²⁰⁵ Andrew Clarke, Andrew M Howe, Jonathan Mitchell, John Staniland, Laurence Hawkes, and Katherine Leeper. Mechanism of anomalously increased oil displacement with aqueous viscoelastic polymer solutions. *Soft Matter*, 11(18):3536–3541, 2015.
- ²⁰⁶ S De, SP Koesen, RV Maitri, M Golombok, JT Padding, and JFM van Santvoort. Flow of viscoelastic surfactants through porous media. *AIChE Journal*, 64(2):773–781, 2018.
- ²⁰⁷ Howard A Barnes. A review of the slip (wall depletion) of polymer solutions, emulsions and particle suspensions in viscometers: its cause, character, and cure. *Journal of Non-Newtonian Fluid Mechanics*, 56(3):221–251, 1995.
- ²⁰⁸ Taha Sochi. Slip at fluid-solid interface. *Polymer Reviews*, 51(4):309–340, 2011.
- ²⁰⁹ Lin Fang, Hua Hu, and Ronald G Larson. Dna configurations and concentration in shearing flow near a glass surface in a microchannel. *Journal of rheology*, 49(1):127–138, 2005.
- ²¹⁰ Hongbo Ma and Michael D Graham. Theory of shear-induced migration in dilute polymer solutions near solid boundaries. *Physics of Fluids*, 17(8):083103, 2005.
- ²¹¹ Rahul Kekre, Jason E Butler, and Anthony JC Ladd. Comparison of lattice-boltzmann and brownian-dynamics simulations of polymer migration in confined flows. *Physical Review E*, 82(1):011802, 2010.
- ²¹² JF Joanny, L Leibler, and PG De Gennes. Effects of polymer solutions on colloid stability. *Journal of Polymer Science: Polymer Physics Edition*, 17(6):1073–1084, 1979.
- ²¹³ Yuki Uematsu. Nonlinear electro-osmosis of dilute non-adsorbing polymer solutions with low ionic strength. *Soft matter*, 11(37):7402–7411, 2015.
- ²¹⁴ Changyong Zhang, Karl Dehoff, Nancy Hess, Mart Oostrom, Thomas W Wietsma, Albert J Valocchi, Bruce W Fouke, and Charles J Werth. Pore-scale study of transverse mixing induced caco3 precipitation and permeability reduction in a model subsurface sedimentary system. *Environmental science & technology*, 44(20):7833–7838, 2010.
- ²¹⁵ Wen Song, Thomas W de Haas, Hossein Fadaei, and David Sinton. Chip-off-the-old-rock: the study of reservoir-relevant geological processes with real-rock micromodels. *Lab on a Chip*, 14(22):4382–4390, 2014.
- ²¹⁶ Rajveer Singh, Mayandi Sivaguru, Glenn A Fried, Bruce W Fouke, Robert A Sanford, Martin Carrera, and Charles J Werth. Real rock-microfluidic flow cell: A test bed for real-time in situ analysis of flow, transport, and reaction in a subsurface reactive transport environment. *Journal of contaminant hydrology*, 204:28–39, 2017.

- ²¹⁷ Chase T Gerold, Amber T Krummel, and Charles S Henry. Microfluidic devices containing thin rock sections for oil recovery studies. *Microfluidics and Nanofluidics*, 22(7):76, 2018.
- ²¹⁸ Sujit S Datta, Harry Chiang, TS Ramakrishnan, and David A Weitz. Spatial fluctuations of fluid velocities in flow through a three-dimensional porous medium. *Physical review letters*, 111(6):064501, 2013.
- ²¹⁹ Amber T Krummel, Sujit S Datta, Stefan Münster, and David A Weitz. Visualizing multiphase flow and trapped fluid configurations in a model three-dimensional porous medium. *AIChE Journal*, 59(3):1022–1029, 2013.
- ²²⁰ Sujit S Datta, Jean-Baptiste Dupin, and David A Weitz. Fluid breakup during simultaneous two-phase flow through a three-dimensional porous medium. *Physics of Fluids*, 26(6):062004, 2014.
- ²²¹ Alexander Groisman and Victor Steinberg. Efficient mixing at low reynolds numbers using polymer additives. *Nature*, 410(6831):905, 2001.
- ²²² Alexander Groisman and Victor Steinberg. Elastic turbulence in curvilinear flows of polymer solutions. *New Journal of Physics*, 6(1):29, 2004.
- ²²³ Christian Scholz, Frank Wirner, Juan Ruben Gomez-Solano, and Clemens Bechinger. Enhanced dispersion by elastic turbulence in porous media. *EPL (Europhysics Letters)*, 107(5):54003, 2014.
- ²²⁴ Firoozeh Babayekhorasani, Dave E Dunstan, Ramanan Krishnamoorti, and Jacinta C Conrad. Nanoparticle dispersion in disordered porous media with and without polymer additives. *Soft Matter*, 12(26):5676–5683, 2016.
- ²²⁵ Soroush Aramideh, Pavlos P Vlachos, and Arezoo M Ardekani. Nanoparticle dispersion in porous media in viscoelastic polymer solutions. *Journal of Non-Newtonian Fluid Mechanics*, 268:75–80, 2019.
- ²²⁶ Teodor Burghlea, Enrico Segre, Israel Bar-Joseph, Alex Groisman, and Victor Steinberg. Chaotic flow and efficient mixing in a microchannel with a polymer solution. *Physical Review E*, 69(6):066305, 2004.
- ²²⁷ YC Lam, HY Gan, Nam-Trung Nguyen, and H Lie. Micromixer based on viscoelastic flow instability at low reynolds number. *Biomicrofluidics*, 3(1):014106, 2009.
- ²²⁸ Phil Ligrani, Daniel Copeland, Chong Ren, Mengying Su, and Masaaki Suzuki. Heat transfer enhancements from elastic turbulence using sucrose-based polymer solutions. *Journal of Thermophysics and Heat Transfer*, 32(1):51–60, 2017.
- ²²⁹ Alain Bourgeat, Olivier Gipouloux, and Eduard Marusic-Paloka. Filtration law for polymer flow through porous media. *Multiscale Modeling & Simulation*, 1(3):432–457, 2003.
- ²³⁰ Ying Diao, Leo Shaw, Zhenan Bao, and Stefan CB Mannsfeld. Morphology control strategies for solution-processed organic semiconductor thin films. *Energy & Environmental Science*, 7(7):2145–2159, 2014.

- ²³¹ Brett G Compton and Jennifer A Lewis. 3d-printing of lightweight cellular composites. *Advanced materials*, 26(34):5930–5935, 2014.
- ²³² Xin Wang, Man Jiang, Zuowan Zhou, Jihua Gou, and David Hui. 3d printing of polymer matrix composites: A review and prospective. *Composites Part B: Engineering*, 110:442–458, 2017.
- ²³³ Min Luo and Iwao Teraoka. High osmotic pressure chromatography for large-scale fractionation of polymers. *Macromolecules*, 29(12):4226–4233, 1996.
- ²³⁴ Siva A Vanapalli, Steven L Ceccio, and Michael J Solomon. Universal scaling for polymer chain scission in turbulence. *Proceedings of the National Academy of Sciences*, 103(45):16660–16665, 2006.